

GROUNDING DESIGN ANALYSIS

A THESIS SUBMITTED TO
THE GRADUATE SCHOOL OF NATURAL AND APPLIED SCIENCES
OF
MIDDLE EAST TECHNICAL UNIVERSITY

BY

MUSTAFA GÜÇLÜ AYDINER

IN PARTIAL FULFILLMENT OF THE REQUIREMENTS
FOR
THE DEGREE OF MASTER OF SCIENCE
IN
ELECTRICAL AND ELECTRONICS ENGINEERING

FEBRUARY 2009

Approval of the thesis:

GROUNDING DESIGN ANALYSIS

submitted by **MUSTAFA GÜÇLÜ AYDINER** in partial fulfillment of the requirements for the degree of **Master of Science in Electrical and Electronics Engineering** Department, **Middle East Technical University** by

Prof. Dr. Canan Özgen
Dean, Graduate School of **Natural and Applied Science** _____

Prof. Dr. İsmet Erkmén
Head of Department, **Electrical and Electronics Engineering** _____

Prof. Dr. Nevzat Özyay
Supervisor, **Electrical and Electronics Engineering Dept., METU** _____

Examining Committee Members:

Prof. Dr. Nevzat Özyay
Electrical and Electronics Engineering Dept., METU _____

Prof. Dr. Arif Ertay
Electrical and Electronics Engineering Dept., METU _____

Prof. Dr. Ahmet Rumeli
Electrical and Electronics Engineering Dept., METU _____

Prof. Dr. Mirzahan Hızal
Electrical and Electronics Engineering Dept., METU _____

Melih Güneri (M.Sc)
AREVA, _____

Date: 10/02/2009

I hereby declare that all information in this document has been obtained and presented in accordance with academic rules and ethical conduct. I also declare that, as required by these rules and conduct, I have fully cited and referenced all material and results that are not original to this work.

Name, Last name:

MUSTAFA GÜÇLÜ AYDINER

Signature :

ABSTRACT

GROUNDING DESIGN ANALYSIS

AYDINER, Mustafa Güçlü.

M.Sc., Department of Electrical and Electronics Engineering

Supervisor: Prof. Dr. Nevzat ÖZAY

February 2009, 104 pages

This thesis investigates problematic cases in AC substation grounding system design. Particularly, the grounding design for substations that are built on high resistivity soil is considered. Here, possible physical rectification schemes are introduced and compared for their effectiveness from safety and cost efficiency perspectives. For this comparison, the CYMGRD program (a finite element analysis tool for AC substation grounding) is used for detailed analysis of the various schemes. An additional computer program is developed to implement the formulations of the related AC substation standards (IEEE, IEE, and Turkish National Regulations). The output of this program is compared with the finite element analysis of the high-resistivity-soil rectification schemes to investigate the validity of the formulations in these standards.

Keywords: AC substation grounding design, ground resistance, grounding grid resistance, fault current, possible design improvements.

ÖZ

TOPRAKLAMA TASARIMI ANALİZİ

AYDINER, Mustafa Güçlü.

Yüksek Lisans, Elektrik-Elektronik Mühendisliği Bölümü

Tez Yöneticisi: Prof. Dr. Nevzat ÖZAY

Şubat 2009, 104 sayfa

Bu çalışma, AC beslemeli şalt sahası topraklamalarının problemlili olanlarını incelemektedir. Özellikle, yüksek özdirençli sahaların topraklamalarının tasarımları üzerinde çalışmalar yapılmıştır. Olası tasarım iyileştirmeleri belirlenmiş ve bu iyileştirmelerin etkinlikleri, güvenlik ve maliyet açılarından incelenmiştir. Bu karşılaştırmalı değerlendirmelerde, CYMGRD programı (FEM analizleri yapan AC topraklama tasarım programı) iyileştirmelerin numerik analizleri için kullanılmıştır. Ayrıca uluslararası (IEEE, IEE) ve yerel (Topraklamalar Yönetmeliği) standartlarda yer alan dört işlem temelli metodlar için bir bilgisayar programı hazırlanmıştır. Yüksek özdirençli sahalar için bu programın sayısal çıktıları ile FEM çıktıları karşılaştırılmış ve metodların güvenilirliği incelenmiştir.

Anahtar sözcükler: AC şalt sahası topraklama tasarımı, topraklama direnci, topraklama ağı direnci, hata akımı, olası tasarım iyileştirmeleri

ACKNOWLEDGEMENTS

I would like to thank Prof. Dr. Nevzat Özey for his valuable guidance and support.

I would like to extend my gratitude also to Melih Güneri for his help on grounding grid design analysis and usage of CYMGRD computer program.

I am grateful to my coordinators Ahmet Ali Uzunalioglu, Oğuzhan Cem and my company METEKSAN SİSTEM for their tolerance during my graduate education.

I wish to express my special thanks to my proposed wife Arzu Erdal and to my brother Can Aydın for their help and support. Also, I wish to express my thanks to my brother Alaeddin , my family Gökhan and Türkan Aydın for their understanding during this study.

TABLE OF CONTENTS

ABSTRACT	iv
ÖZ	v
ACKNOWLEDGEMENTS	vi
TABLE OF CONTENTS	vii
LIST OF FIGURES	x
LIST OF TABLES	xii
LIST OF SYMBOLS	xiii
CHAPTERS	
1. INTRODUCTION	1
1.1. General.....	1
1.2. The Aim and Scope of the Thesis.....	5
2. GROUNDING DESIGN	7
2.1. Grounding Methods.....	7
2.1.1. Conventional Grounding Methods.....	7
2.1.2. Finite Element Grounding Methods.....	22
3. POSSIBLE DESIGN IMPROVEMENTS	26
3.1. General.....	26
3.2. Current in the Grounding Systems	26
3.3. Effects of Soil Treatment.....	34
3.3.1. Soil Treatment by Addition of Electrolytes	36
3.3.2. Soil Treatment by Improving Moisture Retention	36
3.3.3. Soil Treatment by Improving the Contact Surface of the Electrodes	37
3.4. Effects of Rods and Deep-Driven Rods	37
3.5. Explosion Method.....	40
3.6. Parallel Grid Method	43
4. NUMERICAL STUDIES AND SIMULATIONS.....	44

4.1.	Introduction.....	44
4.2.	One Rod Grounding.....	44
4.3.	Mesh Systems	47
4.3.1.	Comparison of Uniform Soil Model Methods	48
4.3.2.	Actual Design Problem 1	51
4.3.3.	Actual Design Problem 2	61
4.3.4.	Actual Design Problem 3	76
4.4.	System Studies.....	77
5.	CONCLUSION	80
A	APPENDIX A	86
A.1	CYMGRD Program.....	86
A.1.1	Program Features.....	86
A.1.2	Analytical Capabilities	86
A.1.3	Screenshots of Data Entry	88
A.1.4	Screenshots of Results.....	90
B	APPENDIX B	92
B.1	Overhead Lines Impedance Z_P Determination	92
C	APPENDIX C	93
C.1	I_G Determination.....	93
C.1.1	Determination of Z_E	93
C.1.2	Determination of I_{Etot}	93
C.1.3	Determination of I_G	94
C.1.4	Determination of GPR.....	94
D	APPENDIX D	95
D.1	Grounding Standards	95
D.2	Utility Practice in Turkey	95
D.3	Effect of Soil Resistivity.....	96
D.3.1	Low Resistivity Case.....	97
D.3.2	High Resistivity Case	97

E	APPENDIX E	98
E.1	Grounding Parameters	98
E.1.1	Tolerable Body Current Limit.....	98
E.1.2	Tolerable Body Voltage Limits.....	99

LIST OF FIGURES

Figure 1.1: Ungrounded system with a line-to-ground fault.....	2
Figure 1.2: Solidly grounded system	4
Figure 2.1: Thapar-gerez predetermined grid shapes	14
Figure 2.2: Wenner four pin method.....	17
Figure 2.3: Example wenner data graph	20
Figure 2.4: Sunde graph	21
Figure 2.5: New finite element model of soil	23
Figure 3.1: Overhead lines impedance model for infinite chain case.	28
Figure 3.2: Overhead lines impedance model for finite chain case	29
Figure 3.3: Line-to-ground fault case in a three station (A, B, C) system	31
Figure 3.4: Total ground impedance	34
Figure 3.5: Effects of moisture, temperature, and chemical content on soil resistivity.....	35
Figure 3.6: Multilayer earth structure	39
Figure 3.7: Relationship between the grounding resistance decreasing role of rods in the two-layer soil	40
Figure 3.8: The explosion method: deep driven tree like electrodes connected to the grounding grid	41
Figure 4.1: Potential distributions of one rod grounding	46
Figure 4.2: Touch potential for one rod grounding.....	46
Figure 4.3: Sample design soil resistivity determination	53
Figure 4.4: Sample grid design	54
Figure 4.5: Potential distributions of sample design.....	55
Figure 4.6: Touch potential distribution of sample design	55

Figure 4.7: Potential distributions of sample design after z_e determination	56
Figure 4.8: Touch potential distribution of sample design after z_e determination	57
Figure 4.9: Soil layers resistivity determination	58
Figure 4.10: Touch potential distribution of sample design after z_e determination with two-layer model	59
Figure 4.11: Potential distributions	60
Figure 4.12: Soil resistivity characteristic curve in two-layer soil model	65
Figure 4.13: Structure of grid design without any enhancement	65
Figure 4.14: Potential distributions from left-bottom corner to right-upper corner.....	67
Figure 4.15: Grid design with additional 40 rods	68
Figure 4.16: Potential distribution with additional 40 rods.....	68
Figure 4.17: Grid design enhanced with 4 deep driven rods.....	70
Figure 4.18: Potential distributions after addition of 4 deep driven rods.....	72
Figure 4.19: Touch potential distribution after overhead lines effect.....	75
Figure 4.20: Potential distributions after overhead lines effect	75
Figure A. 1: Full window screenshot	88
Figure A. 2: Buses.....	88
Figure A. 3: Electrode types.....	89
Figure A. 4: Mat conductor entry.....	89
Figure A. 5: Rod entry	90
Figure A. 6: Soil analysis	90
Figure A. 7: Potential results.....	91
Figure E.1: Step voltage thevenin circuit	101
Figure E.2: Touch voltage thevenin circuit	102
Figure E.3: Tolerable body voltage definitions	104

LIST OF TABLES

Table 2.1: Schwarz method parameters	13
Table 3.1: Geological factor table of explosion method	42
Table 4.1: One rod grounding solutions.....	45
Table 4.2: Resistance calculation results in uniform soil models	49
Table 4.3: Wenner test results for uniform soil problem	52
Table 4.4: Wenner-four-pin test results	62
Table 4.5: Configured test results as average and median values.....	64
Table 4.6: Parallel grid comparison table	79

LIST OF SYMBOLS

Symbol	Description	Clause number
a	Electrode distance in wenner-four-pin method	M
ρ	Soil resistivity	$\Omega \cdot m$
ρ_a	Apparent resistivity from wenner-four-pin tests	$\Omega \cdot m$
ρ_s	Surface layer resistivity	$\Omega \cdot m$
ρ_1	Upper layer resistivity	$\Omega \cdot m$
ρ_2	Lower layer resistivity	$\Omega \cdot m$
S_B	Energy absorbed by body	Joule
$3I_0$	Symmetrical fault current in substation	A
A	Total area enclosed by ground grid	m ²
C_s	Surface layer derating factor	-
d	Rod diameter	M
d_T	Distance between two towers	M
d_{WL}	The geometric mean distance between the earth wire and the line conductors	M
D_F	Far-from-station distance	M
D_f	Decrement factor for determining I_G	-
E_{S50}	Tolerable step voltage for human with 50 kg body	V
E_{S70}	Tolerable step voltage for human with 70 kg body	V
E_{T50}	Tolerable touch voltage for human with 50 kg body	V
E_{T70}	Tolerable touch voltage for human with 70 kg body	V
h	Depth of grid conductors	M
h_s	Height of surface material	M
GPR	Ground potential rise	V
I_B	Body current	A
I_k	Line-to-earth fault current	A
I_G	Current passing through grid	A
I_{Etot}	Total grounding current after reduction factor	A

L_r	Rod length	M
L_P	Peripheral length of grid	M
L_t	Total buried length of conductors without rods	M
L_T	Total buried length of conductors including rods	M
n	Geometric factor composed of n_a , n_b , n_c , and n_d	-
n_R	Number of rods placed in area A	-
r	Rod radius	M
r_{WW}	The earth wire radius	M
\underline{r}	Reduction factor	-
R	Resistance of grounding system	Ω
R_f	Foot resistance of a human	Ω
R_T	Footing resistance of towers	Ω
R'_W	The earth wire per unit length resistance	Ω
S	Separation distance of two rods	M
S_f	Fault current division factor (split factor)	-
t_c	Duration of fault for sizing ground conductor	S
t_f	Duration of fault current	S
t_s	Duration of shock	S
μ_0	Magnetic constant	V·s/A·m
μ_r	The relative permeability of the earth wire	V·s/A·m
ν	The number of earth wires connected to the system	-
ω	Angular frequency	Hz
δ	Equivalent earth penetration depth	-
\underline{Z}_E	Equivalent impedance of system grounding	Ω
\underline{Z}_P	Overhead line impedance	Ω
\underline{Z}_U	Cable shielding and armoring impedance	Ω
\underline{Z}'_W	Earth wire impedance	Ω
\underline{Z}'_{WL}	Mutual impedance per unit length between the earth wire and parallel line conductors	Ω

CHAPTER 1

INTRODUCTION

1.1. General

Although grounding is used for a long time by field engineers, there is a common misunderstanding on the meaning of grounding. Grounding or earthing is normally understood to be the connection of various exposed conductive parts (that are not current carrying under normal circumstances) of equipment together and to a common terminal (main grounding terminal) which is in turn connected by the earthing conductor to an earth electrode. There are two misconceptions in this statement. First, grounding is not only limited to equipment but also involves the electrical power system, the two being related and may refer to the same physical installation in some cases. Second, the term grounding, which is used interchangeably with earthing, is not the same thing. Grounding should be called earthing, only if it involves the physical earth and in case of a mul-functioning of some part of the system, some of the current returns back to the source through the earth. Therefore, the admitted definition of grounding according to [6] is the conducting connection whether intentional or accidental between an electrical circuit or conductive equipment part and a common terminal which is in turn connected by a conductor to an earth electrode or to some conducting body of relatively large extent that serves in place of the earth.

As mentioned above, grounding is divided into two parts as equipment grounding and system grounding. Equipment grounding, referred also as protective

grounding is mainly for the prevention from dangerously high shock that may exist when there is a fault current between an energized electrical conductor and the structure that might either encloses it or is nearby. The system grounding is an intentional electrical interconnection between the electrical system conductors and ground, forming part of the operating system. Main difference between equipment grounding and system grounding is that system grounding is the part of the electrical operating circuit under normal operating conditions while equipment grounding is not. Objectives behind the system grounding are to fix the potential at any part of the network with respect to earth and to provide sufficient fault current so that protection equipment can operate. System grounding can be of four different types, which are ungrounded systems, resistance grounding, reactance grounding and solid grounding.

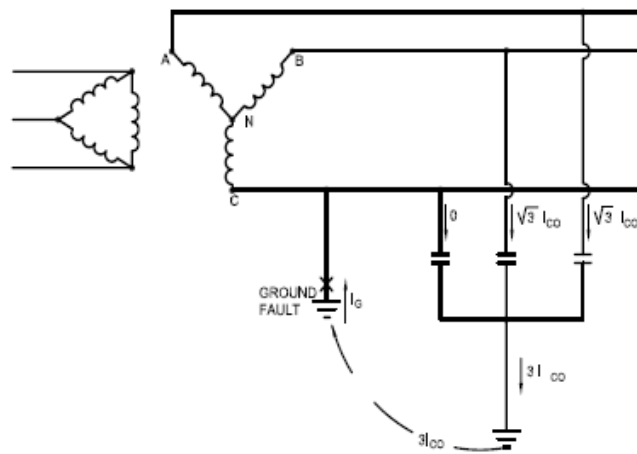


Figure 1.1: Ungrounded system with a line-to-ground fault

There is no connection between earth and the system neutral except for very high impedance devices in ungrounded systems. Even if the system is not grounded, the system is still coupled to ground through the distributed capacitances (Figure

1.1). By this way, system fixes the neutral point and the voltages are not floating. Such systems are defined as ungrounded systems. The problem with this type of system is that there is only the ground capacitance current, which makes detection by over current relays impossible in case of line-to-ground fault, and potential of the other phases raise to line-to-line voltage levels. This will over-stress the insulation of healthy phases so that likely-hood of a second line-to-ground fault is increased. These are the main disadvantages of this type of systems. On the other hand, as an advantage, system goes on operating when line-to-ground fault takes place.

Resistance and reactance grounded systems employ an intentional resistance or impedance connection between the neutral of the system and ground. Although, these systems provide fault current, the high voltage is still experienced on healthy phases in case of a ground fault. Fault current can be limited to acceptable levels 1-1000A in case of a low resistance grounding or miliampers in case of a high resistance grounding, which is similar to ungrounded systems. Reactance grounding is not normally preferred for distribution systems because low resistance grounding has better reduction on ground fault current compared to reactance grounded systems.

High voltage (HV) systems are usually solidly-grounded (Figure 1.2). In this case, there is no intentional impedance between the system neutral and the ground (earth). Under these circumstances, the ground fault current can reach to very high levels. These systems are normally made up of overhead lines and, therefore, there is no problem with the stress of high fault currents. However, insulation is a problem in high voltage systems. In solidly grounded systems, the voltage across the healthy phases do not increase with the occurrence of a line-to-ground fault. The fault currents are limited by Turkish national regulations (APPENDIX D), which are 50kA for 380kV systems and 31.5kA for 154kV systems.

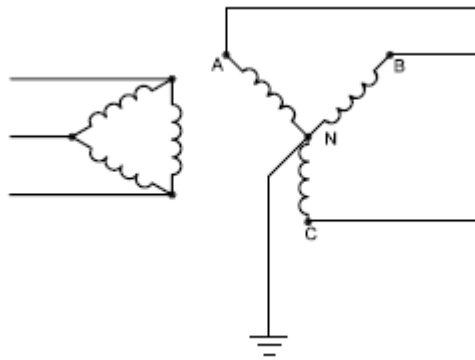


Figure 1.2: Solidly grounded system

When such high currents flow into the earth, the potential at the point of contact to earth will increase to dangerous levels. For example, a ground fault current of 25kA going through a ground resistance of 1Ω will rise the potential to 25kV at the grounded point, which is harmful to both human and equipment in a grounding region. This voltage is known as the ground potential rise (GPR) which is the most important parameter for designing grounding systems. GPR is defined as the maximum electrical potential that substation grounding may reach relative to a distant grounding point. This potential has to be limited to a value such that it is not hazardous to system operation. For this purpose, maximum GPR values are taken to be 20kV for 154kV HV systems and 31.5kV for 380kV systems as design criteria in Turkey. Further, GPR is directly proportional to both the grounding resistance (R) and the maximum grid current (I_G). Therefore, in case of a high GPR design problem, possible design improvements that are capable of reducing either grounding resistance or maximum grid current can be applied for GPR minimization.

Along with system operation, another important aim in grounding designs is to protect people and equipments against harmful overvoltages. In case of a grounding design, considered parameters (APPENDIX E) are step and touch

potentials. The step potential [2] is the difference in surface potential experienced by a person bridging a distance of 1m with the feet without contacting any grounded object. On the other hand, the touch potential [2] is defined as the potential difference between the ground potential rise (GPR) and the surface potential at the point where a person is standing while at the same time having a hand in contact with a grounded structure. These potentials are not to be exceeded their maximum permissible levels to protect human life and equipments.

1.2. The Aim and Scope of the Thesis

The aim of the thesis is to design grounding systems such that, in case of high fault currents, the acceptable levels of step and touch potentials are held below their maximum permissible levels. These designs were possible for the conventional outdoor substations that cover usually very large areas. However with the introduction of gas insulated substations (GIS), which require an area of approximately $1/10^{\text{th}}$ of the area required by conventional outdoor substations, it is hard to reduce grounding resistance. In addition, if the soil resistivity of the region is high, then the problem of reducing grounding resistance become more difficult. Therefore, the focus of the thesis is to investigate the techniques, which are capable of reducing grounding resistance to acceptable values. In the final grounding design, the designer's primary duty is ensuring the safety of living things in the vicinity of the AC substation, in particular human beings. Further, the design has to enhance the safety of the power equipment in the grounded area while aiding the system operation by clearing faults. Finally, the design has to be made in a cost effective way.

In Chapter 2, the conventional methods of grounding systems such as rods, uniform soil grids are discussed. Formulas that have been developed ([1-4, 9-13]) to calculate the effective ground resistance, are discussed and finite element method (FEM) for calculating the ground resistance and GPR is introduced.

In those cases, where acceptable grounding designs have to be designed under difficult conditions, the methods given in Chapter 2 may not be sufficient. The techniques, which will enhance these methods, are discussed in Chapter 3. In this chapter, it is shown that the starting point of a grounding design is the determination of the part of the fault current going through the grounding system. If this is not done properly, over-sized grounding systems will result. This is analyzed in detail.

In Chapter 4, the effectiveness of the designs discussed in previous two chapters are compared. This is done with a professional ground resistance simulation program, CYMGRD, which is discussed in APPENDIX A.

Finally, in Chapter 5, concluding remarks and the future work that needs to be done, are given.

CHAPTER 2

GROUNDING DESIGN

Identifying the resistance to ground is a major point and it is mostly dependant on soil resistivity of the area to be grounded. There are multiple alternative methods for the designer to reduce grounding resistance. These alternatives are given next and are listed from simplest to complex. In each alternative either used equipment is considered in equations or soil models are determined for grounding resistance determination.

2.1. Grounding Methods

Alternative grounding methods can be classified into two groups as conventional methods and finite element methods. In the following sections, these methods are introduced.

2.1.1. Conventional Grounding Methods

a- One rod grounding design methods

If there is an electrode in the ground, the resistance to ground depends on the soil resistivity. Assume, one use a rod as an electrode located in the ground with a certain soil type. Many researchers studied on one rod grounding and they found

different empirical equations to calculate ground resistance. Three of these methods are taken from references in the order of [1], [9] and [10].

I. Method 1

$$R = \frac{\rho}{2\pi C} \quad (2-1)$$

where R is resistance in Ω , ρ is soil resistivity in $\Omega\cdot\text{cm}$, C is electrostatic capacitance (computed by Eq. (2-2)) of one rod in Farads. Electrostatic capacitance of one rod is given by the following formula.

$$C = \frac{13.25L_r}{1.55 + \log\left(\frac{L_r}{d}\right)} \quad (2-2)$$

where L_r is rod length in feet, d is rod diameter in inches.

By putting the computed electrostatic capacitance into Eq. (2-1), one can obtain resistance to ground value of a one rod grounding by knowing soil resistivity, rod length and rod diameter. For more detailed information refer to [1].

II. Method 2

Ground resistance of one rod or pipe grounding can be computed by Eq. (2-3).

$$R = \frac{100\rho}{2\pi L_r} \times \left(\ln \frac{8L_r}{d} - 1 \right) \quad (2-3)$$

where ρ is soil resistivity in $\Omega\cdot\text{m}$, L_r is rod length in cm, d is rod diameter in cm.

In this method, the diameter of copper rods recommended between 13mm and 19mm. Also length of copper rods recommended between 1,22m and 2,44m.

III. Method 3

This method is the most commonly used equation (given in Eq. (2-4)) for single rod grounding, which is developed by Prof. H. R. Dwight and called as Dwight method.

$$R = \frac{\rho}{2\pi L} \times \frac{\{(\ln 4L_r) - 1\}}{r} \quad (2-4)$$

where ρ is soil resistivity in $\Omega\cdot\text{m}$, L_r is rod length in cm, r is rod radius in cm.

b- Two rods system grounding method

If there are two electrodes in the ground, which are separated with a distance S , electrostatic capacitance given in Eq. (2-5) is valid.

$$C = \frac{61L_r}{3.56 + 2.3 \log\left(\frac{L_r}{d}\right) + \frac{L_r}{S} + \frac{1}{3}\left(\frac{L_r}{S}\right)^3 + \frac{2}{5}\left(\frac{L_r}{S}\right)^5} \quad (2-5)$$

By computing the capacitance of two rods from Eq. (2-5) and putting it in Eq. (2-1), one can obtain resistance to ground value of two rods grounding by knowing soil resistivity, rod length and rod diameter [1].

c- Multi-rods system grounding

There is no specialized method to compute grounding resistance of a multi-rods system. In this kind of systems, only computation way to measure grounding resistance is using finite element analysis —introduced in section 2.1.2 Finite Element Grounding Methods —.

d- System grounding with grids in uniform soil conditions

Grounding grid is an intermeshed network of conductors which are located under the area which requires control of potential caused by a fault current. Resistance to ground calculation method for a uniform soil covered by a grounding grid region used to be studied by many researchers. IEEE 80-2000 [2] includes and defines some methods. Commonly used methods are Laurent-Niemann Method, Sverak Method, Schwarz Method and Thapar-Gerez Method.

I. Laurent-Niemann Method

The ground resistance is a function of the area covered by the substation and the soil resistivity in the substation region. The soil resistivity has a non-uniform nature. It is a well-known fact that soil resistivity may vary both vertically and horizontally in an earth region. Varying soil resistivity causes varying resistance from the direct relation between soil resistivity and resistance. So the designer try to estimate the minimum value of ground resistance at a certain depth h from the ground surface. Laurent-Niemann Method expressed Eq. (2-6) to estimate the ground resistance.

$$R = \frac{\rho}{4} \sqrt{\frac{\pi}{A}} + \frac{\rho}{L_T} \quad (2-6)$$

where A is area covered by the substation in m², L_T is total buried length of conductors.

L_T formulation is taken from IEEE 80-2000 [2] and given in Eq. (2-7).

$$L_T = L_t + n_R \cdot h \quad (2-7)$$

where L_t is total length of conductors in grid in m, n_R is number of grounding rods used in grid in m, h is the depth of the grid in m.

From the examination of Eq. (2-6), left side of the summation is for calculating ground resistance at the surface of the soil and right side of the summation is for calculating ground resistance of the total buried length of the conductors. Summation leads the formulation to ground resistance R in Ω.

II. Sverak Method

This method can be called as the integrated form of Laurent-Niemann Method. Ground resistance at the surface of the soil is modified in order to improve the accuracy of the ground resistance calculated. Researchers observed significant effect of the grid depth on ground resistance and decided that this effect is large enough to be included it to the equation. Therefore, Eq. (2-6) is rearranged and the resultant Eq. (2-8) is obtained.

$$R = \rho \left[\frac{1}{L_T} + \frac{1}{\sqrt{20A}} \left(1 + \frac{1}{1 + h\sqrt{20/A}} \right) \right] \quad (2-8)$$

Examining Laurent-Niemann and Sverak Equations, it can be easily understood that the resistance is directly proportional to resistivity and inversely proportional to total buried length of conductors. Resistance is also inversely proportional to

square root of area. Therefore, the following observations can be derived. First such observation is that increasing area of grounding grid decreases the resistivity in the order of square-root. Sometimes this is possible in real life. If the land is not costly for grounding grid design region, increasing area will lead to a feasible solution. However, in residential areas, land is expensive and limited. Second observation is that ground resistance decreases while using more conductors in grid designs. Although, increasing the total buried length of conductors seems to be leading a desired ground resistance in grounding grid designs, desired solution won't be feasible enough because such conductor material, copper is very expensive. Reference [3] has derivation of Eq. (2-8) and further information about Sverak Method.

III. Schwarz Method

Schwarz developed following set of equations in order to determine the grounding resistance in uniform soil conditions. Schwarz equations are composed of three equations and one equation for merging the three.

Main equation merging the other three equations is given in Eq. (2-9).

$$R = \frac{R_1 R_2 - R_m^2}{R_1 + R_2 - 2R_m} \quad (2-9)$$

where, R_1 , R_2 , R_m are determined by three different equations. R_1 is determining the ground resistance of a grid formed by straight horizontal wires and represented in Eq. (2-10).

$$R_1 = \frac{\rho}{\pi L_t} \left[\ln \left(\frac{2L_t}{a'} \right) + \frac{k_1 L_t}{\sqrt{A}} - k_2 \right] \quad (2-10)$$

where ρ is the soil resistivity in $\Omega \cdot m$, L_t is the total length of all connected grid conductors in m, $2a$ is the diameter of conductor in m, a' is $(a \cdot 2h)^{1/2}$ for conductors

buried at depth h , or a' is a on earth surface, A is the area covered by conductors in m^2 , k_1 and k_2 are the coefficients found by the following equations according to the value of grid depth (h).

The values of k_1 and k_2 in Eq. (2-10) are given in Table 2.1 for different values of the grid depth. In the formulations x is given as the length to width ratio of grid.

Table 2.1: Schwarz method parameters (h , k_1 and k_2)

h	k_1	K_2
0	$-0.04x + 1.41$	$0.15x + 5.50$
$1/(10A^{1/2})$	$-0.05x + 1.20$	$0.10x + 4.6$
$1/(6A^{1/2})$	$-0.05x + 1.13$	$-0.05x + 4.40$

In Eq. (2-11), R_2 determines the ground resistance of a rod bed.

$$R_2 = \frac{\rho}{2\pi n_R L_r} \left[\ln\left(\frac{4L_r}{b}\right) - 1 + \frac{2k_1 L_r}{\sqrt{A}} \left(\sqrt{n_R - 1}\right)^2 \right] \quad (2-11)$$

where L_r is the length of each rod in m, $2b$ is the diameter of rod in m, n_R number of rods placed in area A .

The third variable in Schwarz Equation is given in Eq. (2-12). R_m is the combined ground resistance of the grid and the rod bed.

$$R_m = \frac{\rho}{\pi L_t} \left[\ln\left(\frac{2L_t}{L_r}\right) + \frac{k_1 L_t}{\sqrt{A}} + 1 - k_2 \right] \quad (2-12)$$

One can obtain the grounding grid resistance by computing k_1 , k_2 , R_1 , R_2 , R_m in the given order and putting the calculated values in Eq. (2-9). Reference [4] has the necessary derivations to obtain Schwarz equations.

IV. Thapar-Gerez Method

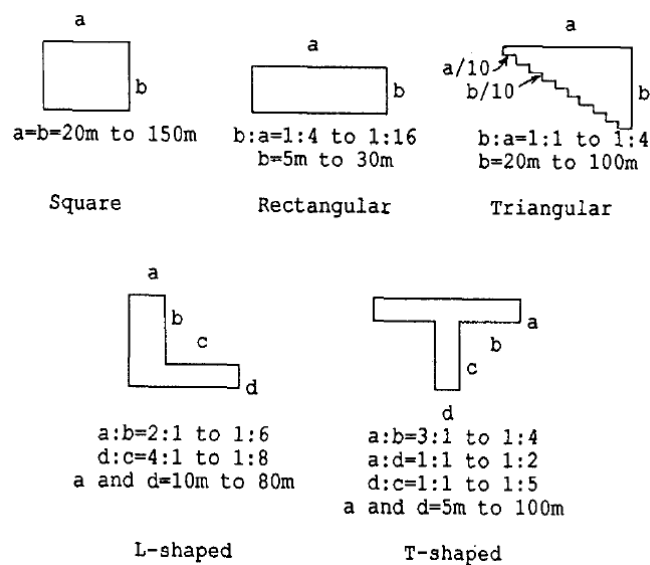


Figure 2.1: Thapar-gerez predetermined grid shapes ([5])

Thapar and Gerez worked on a complex computer program, which is based on finite element analysis in order to determine resistance of a grounding system made of straight linear conductors laid in three mutually perpendicular directions. Thapar and Gerez determined ground resistances of more than 100 grids which have different shapes, configurations and sizes by using their program. They developed an empirical equation which is valid for their predetermined grid shapes and configurations for varying sizes. Predetermined grid configurations are given in Figure 2.1.

In Eq. (2-13), Thapar-Gerez formula is given and this formula is the integrated version of Eq. (2-8). In detail, an extra multiplication part is added to include the effect of grounding region shapes on calculated resistance.

$$R = \rho \left[\frac{1}{L_T} + \frac{1}{\sqrt{20A}} \left(1 + \frac{1}{1 + h\sqrt{20/A}} \right) \right] * 1.52 \left[2 \ln(L_p \sqrt{2/A}) - 1 \right] \frac{\sqrt{A}}{L_p} \quad (2-13)$$

where L_p is the peripheral length of grid.

Thapar-Gerez equation is dimensionless and does not change according to the shape of the grid. Also it is based on the factor \sqrt{A}/L_p . This factor comes from the known fact that ground resistance of a conductor of given surface area decreases as the length over which the area spreads is increased.

All of these four methods assume solutions in uniform soil models. Also all four methods are inversely proportional to primary parameters such as length of total conductors (L_T) used in grid and area covered by the grid (A). Differences of these methods are the secondary parameters used such as depth of grid (h), diameter of conductor ($2a$), rod diameter ($2b$), and rod length (L_r). Numerical comparisons and simulations are given in section 4.3.1 Comparison of Uniform Soil Model Methods.

e- Two layer or multilayer system grounding

Highly non-uniform soil characteristics may be encountered from Wenner Test results of the grounding design region. In such soil conditions, both two layer and multilayer soil models can be used. Multilayer soil models can be used if and only if there does not exist a feasible two-layer equivalent design according to [2]. A multilayer soil model includes several horizontal soil layers. Techniques to

interpret highly non uniform soil resistivity require the use of computer programs or graphical methods developed by the researchers. As it is given in [2], that in most cases, the grounding regions can be modeled, based on an equivalent two-layer model that is sufficient for designing a safe grounding system. For further information on details of multilayer model calculations, [2] gives adequate information. Multilayer model is not discussed in this study whereas details of two-layer soil model calculations are given next.

Two layer soil models can be designed in three different ways:

- Determination of an earth model by minimizing error function
- Determination of an earth model by graphical data
- Determination of an earth model by finite element model

I. Determination of an earth model by minimizing error function

Earth characteristics are measured using test methods. For this purpose, Wenner-four-pin method is widely used. Soil resistivity can be determined by Eq. (2-14) from test results. All test methods used in grounding and their samples are given in [11].

$$\rho = \frac{4\pi aR}{1 + \frac{2a}{\sqrt{a^2 + 4b^2}} - \frac{a}{\sqrt{a^2 + b^2}}} \quad (2-14)$$

where a is electrode distance in m, b is electrode depth in m, R is measured value in Ω .

Wenner-four-pin method structure is given in Figure 2.2.

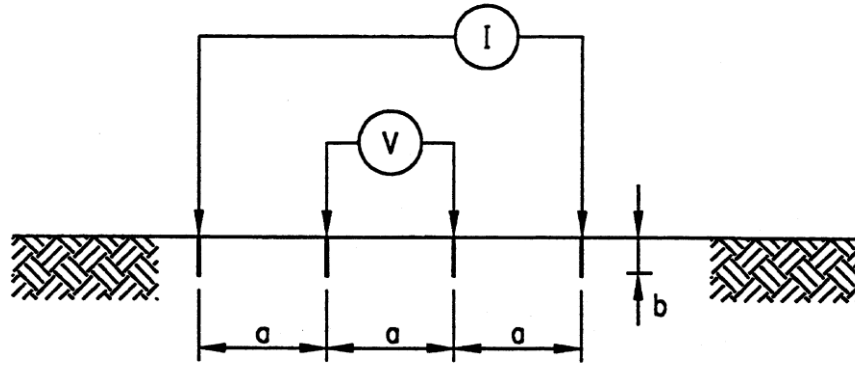


Figure 2.2: Wenner four pin method ([2])

For different values of a —electrode distance—, Wenner-four-pin method is repeated in the diagonal length of the area to be modeled. Different resistance (R) values are determined, so different values of resistivity (ρ) are determined. In order to model these tests in two layer soil model, two layer soil apparent resistivity has to be calculated for these different tests.

Eq. (2-15) introduces the formulation of the apparent resistivity (ρ^0).

$$\rho^0 = \rho_1 \left[1 + 4 \sum_{n=1}^{\infty} \frac{K^n}{\sqrt{1 + \left(2n \frac{h}{a}\right)^2}} - \frac{K^n}{\sqrt{4 + \left(2n \frac{h}{a}\right)^2}} \right] \quad (2-15)$$

where ρ_1 is the resistivity near the surface (upper layer) in two layer soil model in $\Omega \cdot m$, ρ_2 is the resistivity going through the depth (lower layer) in two layer soil model in $\Omega \cdot m$, n varies in $1 - \infty$ (number of test attempts), h is the upper layer depth in m , a is the electrode distance in m . K is the reflection factor and can be computed from Eq. (2-16).

$$K = \frac{\rho_2 - \rho_1}{\rho_2 + \rho_1} \quad (2-16)$$

In two layer soil model, error function is defined as $\psi(\rho_1, K, h)$.

$$\psi(\rho_1, K, h) = \sum_{m=1}^N \left[\frac{\rho_m^0 - \rho_m}{\rho_m^0} \right]^2 \quad (2-17)$$

where N is the total number of measured resistivity values, a is the electrode spacing.

By minimizing the error function, one can obtain best fit ρ_1 , K, h values. In other words, soil resistivities can be determined. Steepest descent —equations are reproduced from [11] — is one of the minimization methods and can be used to minimize the error function given in Eq. (2-17). For this purpose from Eq. (2-18) to Eq. (2-22), usage of steepest descent method is explained.

Gradient of Error function is given in Eq. (2-18).

$$\Delta\psi = \left(\frac{\partial\psi}{\partial\rho_1} \right) \Delta\rho_1 + \left(\frac{\partial\psi}{\partial\rho_2} \right) \Delta\rho_2 + \left(\frac{\partial\psi}{\partial h} \right) \Delta h \quad (2-18)$$

Differential equations, that are present in Eq. (2-18), can be derived as in Eq. (2-19) respectively.

$$\begin{aligned}
\frac{\partial \psi}{\partial \rho_1} &= -2 \sum_1^N \left[\frac{\rho^0 - \rho}{\rho^0} \right] \frac{\partial \rho}{\partial \rho_1} \\
\frac{\partial \psi}{\partial \rho_2} &= -2 \sum_1^N \left[\frac{\rho^0 - \rho}{\rho^0} \right] \frac{\partial \rho}{\partial \rho_2} \\
\frac{\partial \psi}{\partial h} &= -2 \sum_1^N \left[\frac{\rho^0 - \rho}{\rho^0} \right] \frac{\partial \rho}{\partial h}
\end{aligned} \tag{2-19}$$

Field engineers have to be sure that the calculation converges to a solution with desired accuracy. So τ , σ , γ values given in Eq. (2-20) should be chosen to be positive and small enough so that gradient of error function can converge.

$$\begin{aligned}
\Delta \rho_1 &= -\tau \frac{\partial \psi}{\partial \rho_1} \\
\Delta \rho_2 &= -\sigma \frac{\partial \psi}{\partial \rho_2} \\
\Delta h &= -\gamma \frac{\partial \psi}{\partial h}
\end{aligned} \tag{2-20}$$

Let ρ demonstrate resistivity calculated from Wenner method. Eq. (2-21) can be derived from Eqs. (2-18) and (2-20).

$$\Delta \psi = -\tau \left(\frac{\partial \psi}{\partial \rho_1} \right)^2 - \sigma \left(\frac{\partial \psi}{\partial \rho_2} \right)^2 - \gamma \left(\frac{\partial \psi}{\partial h} \right)^2 \tag{2-21}$$

By assuming initial values for ρ_1 , ρ_2 and h , the error function can be iterated over values in Eq. (2-22) until the error function approaches a desired error value.

$$\begin{aligned}
\rho_1^{(k)} &= \rho_1^{(k-1)} + \Delta \rho_1 \\
\rho_2^{(k)} &= \rho_2^{(k-1)} + \Delta \rho_2 \\
h^{(k)} &= h^{(k-1)} + \Delta h
\end{aligned} \tag{2-22}$$

As a result, a grounding area can be modeled using two layer soil model by obtaining ρ_1 , ρ_2 , and h from minimization of error function. Reference [11] includes sample computation of this method.

II. Determination of an earth model by graphical data

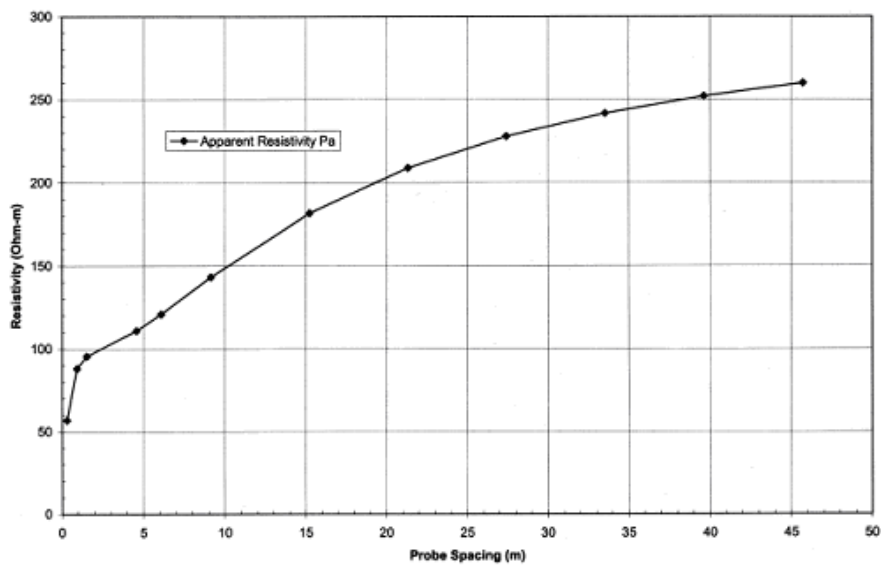


Figure 2.3: Example wenner data graph ([2])

One can obtain the soil characteristics of a region in two layer soil model by using graphical methods. Many researchers study on these methods to investigate an easy way for soil resistivity determination whereas usage of these methods require accurate and close enough Wenner-four-pin test results to apply, that is not possible in most cases. Sunde graphical method is introduced next. [2] include necessary information in order to find studies of other researchers on this subject.

Sunde method composed of several steps as follows:

- Wenner four pin method tests are applied to the area to be grounded.
- Plot a graph from the test data such as given in Figure 2.3. Vertical axis of graph is resistivity ρ in $\Omega\cdot\text{m}$ and horizontal axis of graph is probe spacing a in m.
- Estimate ρ_1, ρ_2 from the plotted graph in step above. Upper limit of the graph is estimated as ρ_2 and lower limit of the graph is estimated as ρ_1 .
- Calculate ρ_2 / ρ_1 and use this value in Sunde graph (given in Figure 2.4) as selecting the matched plot or drawing a matching plot on the same graph.
- Select the value ρ_a / ρ_1 on y-axis within the sloped region of the appropriate ρ_2 / ρ_1 curve in Figure 2.4.

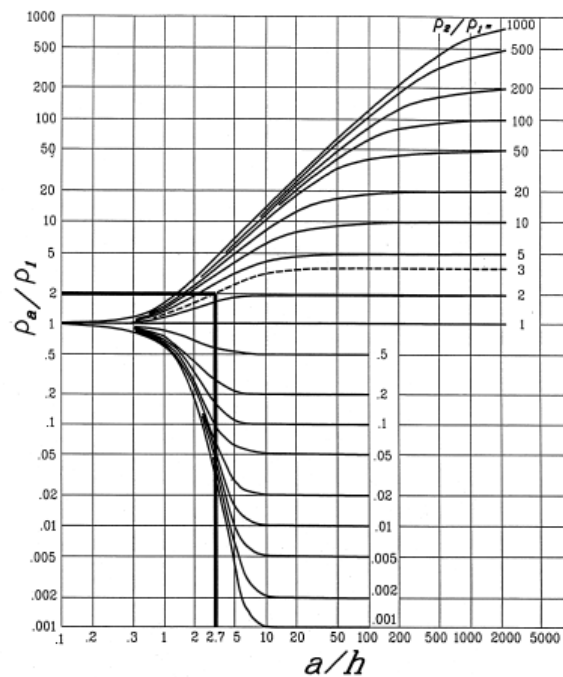


Figure 2.4: Sunde graph ([2])

- Read the corresponding value in x-axis for a / h ratio.
- Compute ρ_a from ρ_a / ρ_1 value.
- Read the probe spacing a (illustrated in Figure 2.2) by using computed ρ_a .
- By using a, find h from a / h ratio found.

III. Determination of an earth model by finite element model

Finite element analysis, which is used in determination of ground resistance, is capable of both one rod or multi rod grounding and uniform or non-uniform soil models grounding computations. Therefore, detailed analysis of finite element methods is given in section 2.1.2 Finite Element Grounding Methods.

In non-uniform resistivity soil conditions, using two layer soil model or multilayer soil model is essential. Two layer soil model simulations and comparisons are discussed in section 4.3 Mesh Systems.

2.1.2. Finite Element Grounding Methods

Most recent studies about grounding analysis are based on Finite Element Methods (FEM). FEM used to determine grounding resistance of a design or a grounded region. They give more accurate results compared to conventional grounding methods discussed in section 2.1.1 Conventional Grounding Methods.

Old FEM methods are composed of current flow analysis by using grid potential set. After the current is computed, ground resistance can be found by dividing voltage by current. In this method, main disadvantage is selecting the size of the model such as earth distance to be considered is starting from the grounding grid. Since analysis of each potential in the soil for a selected point is considered from grounding grid to the point.

New FEM methods are developed by researchers such as main disadvantage of old FEM method is overcome. They model the problem from the beginning. In the first step, they assume that grounding resistance is such a parameter that does not depend on potential or current in the grid except frequency cases other than power frequencies (50Hz or 60Hz). Second assumption is that the region is an infinite flat surface. ([13] give sample results and derivations). Model structure for this solution is given in Figure 2.5.

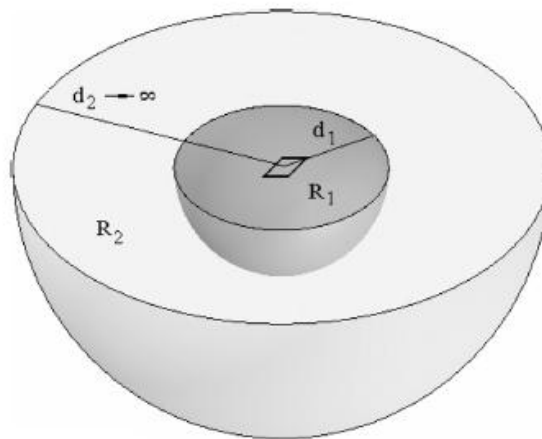


Figure 2.5: New finite element model of soil ([13])

R_1 , R_2 , d_1 and d_2 are the variables for the model where d_1 is the distance from grid to the points where semi-spherical model of equipotent surface disturbs, d_2 is the distance from grid to the points where electrical potential goes to zero. Technically, this point is at infinity. R_1 is the resistance inside the semi-spherical surface and R_2 is the resistance outside the semi-spherical surface.

From tests of various designs, researchers found that Eq. (2-23) can be used to determine d_1 [13].

$$d_1 = \frac{D}{2} + 30 \quad (2-23)$$

where D is the diagonal distance of grounding grid.

Resistance of grounding grid given in Eq. (2-24) can be derived easily from Figure 2.5.

$$R = R_1 + R_2 \quad (2-24)$$

In [13], R_2 is computed from Eq. (2-25).

$$R_2 = \frac{\rho}{2\pi d_1} \quad (2-25)$$

Determination of R_1 is not as simple as R_2 . This is where finite element analysis exactly takes its place. In general, R_1 can be calculated from dissipated power given in Eq. (2-26).

$$R_1 = \frac{(\text{Voltage})^2}{\text{Dissipated Power}} \quad (2-26)$$

R_1 can be detailed by replacing the terms as in Eq. (2-27).

$$R_1 = \frac{(V_G - V_B)^2}{\int_V \frac{E^2}{\rho} dV} \quad (2-27)$$

where V_G is the potential in the grid, V_B is the potential in the boundary d_1 .

From Eqs. (2-25) and (2-27), one can compute the grid resistance by Eq. (2-24). Finite Element Analysis can be also used for determining touch and step voltages. Once R is determined from FEM, step and touch voltages can be determined by the help of following steps.

Actual grid potential (V_{AG}) is determined by Eq. (2-28) by finite element analysis.

$$V_{AG} = R \cdot I_G \quad (2-28)$$

where I_G is actual fault current in A.

Actual boundary potential (V_{AB}) is determined by Eq. (2-29) by finite element analysis.

$$V_{AB} = R_2 \cdot I_G \quad (2-29)$$

Once all potential distribution is computed, from nodal potential differences one can obtain step and touch voltages. Further information is given in [12] and [13].

CHAPTER 3

POSSIBLE DESIGN IMPROVEMENTS

3.1. General

For most substations, it is possible to design a satisfactory grounding system provided that the earth resistance is low; i.e. in the range 10-400 $\Omega\cdot\text{m}$. In these cases, conventional grounding techniques can be utilized to get the desired levels of grounding. However, if the earth resistance is excessive, i.e. larger than 400 $\Omega\cdot\text{m}$, then special techniques are required to obtain the low resistance grounding. Further, if the substation is GIS type, where area covered is smaller when compared to conventional outdoor substations, it comes out to be more difficult to have an effective and acceptable grounding resistance value.

In the following sections, special methods, which would enhance the effect of conventional design techniques, are discussed and analyzed. The numerical comparisons obtained will be given in the following chapter.

3.2. Current in the Grounding Systems

The utility practices in Turkey (APPENDIX D) given for the short circuit currents are 50kA for 380kV systems and 31.5kA for 154kV systems. These values are the ultimate short-circuit levels and the present values are very much lower. On the other hand, the grounding systems designed for these voltage levels are 35 kA at 380 kV systems and 20 kA for 154 kV systems. This is due to the fact that some

of the fault current is diverted to the ground wires of the transmission lines, and therefore the current going through the substation grounding will be smaller. This reduction factor is taken to be 0.65 independent of the number of transmission lines terminating at the substation. In addition, effect of overhead lines entering the substation is omitted in the fault current division in determination of current.

When a fault takes place in the vicinity of one of the grounding grids, the connections (overhead line grounding wires, cable shielding and armoring) to the other grounding grids participate in clearing the fault current. Accordingly, the first step of the design strategy is calculating the exact fault current that needs to be cleared by the high-resistivity-soil grounding grid (to satisfy the ultimate criteria on step voltage, touch voltage and GPR). This calculation is system-specific and accounts for the current that is cleared by the connections to the surrounding grounding grids. The end result is a safe design for the high-resistivity-soil grounding grid despite the fact that its computed fault current is less than the Turkish regulation values (recall, for these values, a design is not even possible).

In the following analysis, overhead line effects on fault current that is carried through the overhead line earth wire is discussed. Then, by the help of the overhead line effect, computation of overhead-line-reduction-factor (that is a factor that represents the reduction because of the mutual impedance effect between earth wires and parallel phase conductors), current division factor (which represents part of the fault current passing through the grounding grid) and decrement factor (that accounts the effect of initial dc offset and its attenuation during the fault) will be introduced to compute the fault current that flows through the grounding grid [18].

Figure 3.1 shows a sample overhead line structure for infinite number of earth wires. The equivalent impedance seen from one end of the infinite chain overhead line is called as the driving point impedance (Z_P).

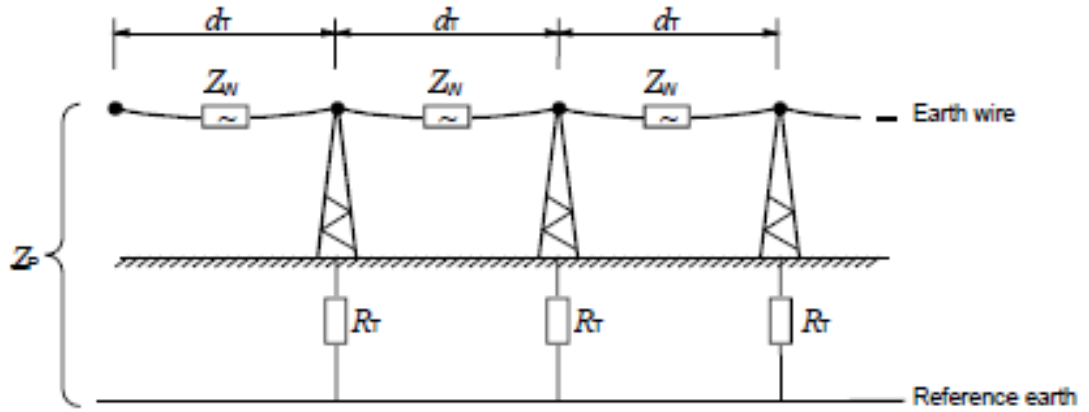


Figure 3.1: Overhead lines impedance model for infinite chain case. ([18])

The infinite chain formulation for \underline{Z}_P [18] yields

$$\underline{Z}_P = 0.5\underline{Z}_W + \sqrt{(0.5\underline{Z}_W)^2 + \underline{Z}_W R_T} \quad (3-1)$$

where \underline{Z}_W is the earth wire impedance between two towers, and R_T is the footing resistance of towers at a distance of d_T . The validity of the infinite chain assumption is found by computing, far-from-station distance (D_F). If the distance between the substation that has the fault and the nearby station connected with overhead lines is bigger than D_F computed from Eq. (3-2), infinite chain formulation can be used and vice versa.

$$D_F = 3\sqrt{R_T} \frac{d_T}{\text{Re}\{\sqrt{\underline{Z}_W}\}} \quad (3-2)$$

According to the validity of infinite chain assumption, if the chain of towers cannot be assumed to be infinite, the following Eq. (3-3) is utilized for n towers. The new structure composed of finite number of overhead lines is given in Figure 3.2.

$$\underline{Z}_P = \frac{\underline{Z}_P(\underline{Z}_{EB} + \underline{Z}_P) \cdot \underline{k}^n + [\underline{Z}_P(\underline{Z}_{EB} - \underline{Z}_P + 2\underline{Z}_W) - \underline{Z}_W(\underline{Z}_{EB} + \underline{Z}_W)] \cdot \underline{k}^{-n}}{\underline{Z}_P(\underline{Z}_{EB} + \underline{Z}_P) \cdot \underline{k}^n - (\underline{Z}_{EB} - \underline{Z}_P + \underline{Z}_W) \cdot \underline{k}^{-n}} \quad (3-3)$$

where \underline{Z}_{EB} is the earth impedance of an outer substation that is located at the end of the overhead line and is called as B in Figure 3.2 and \underline{k} is given by

$$\underline{k} = 1 + \underline{Z}_W \left(\frac{1}{R_T} + \frac{1}{\underline{Z}_P} \right) \quad (3-4)$$

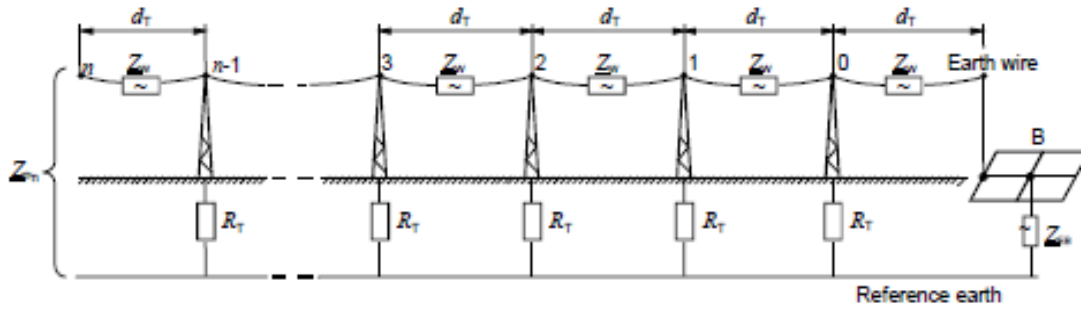


Figure 3.2: Overhead lines impedance model for finite chain case ([18])

The determination of the earth wire impedance (\underline{Z}_W) between two towers at a distance of d_T is given by [18]

$$\underline{Z}_W = \underline{Z}'_W \cdot d_T \quad (3-5)$$

where \underline{Z}'_w is defined as per unit length earth-wire impedance with earth return. \underline{Z}'_w is formulated by Eq. (3-6).

$$\underline{Z}'_w = R'_w + \frac{\omega\mu_0}{8} + j\omega\frac{\mu_0}{2\pi} \left[\frac{\mu_r}{4\nu} + \ln \frac{\delta}{r_{ww}} \right] \quad (3-6)$$

where R'_w is the earth wire per unit length resistance, μ_0 is the magnetic constant, μ_r is the relative permeability of the earth wire, ν is the number of earth wires connected to the system, r_{ww} is the earth wire radius (for one earth wire value is r_w , for two earth wires value is $(r_w \cdot d_w)^{1/2}$), d_w is the distance between two earth wires, and δ is the equivalent earth penetration depth determined by Eq. (3-7).

$$\delta = \frac{1.85}{\sqrt{\frac{\omega\mu_0}{\rho}}} \quad (3-7)$$

According to [18], similar approach may be introduced to determine cable shielding and armoring impedance, \underline{Z}'_U . Although cable effect is investigated in detail [27-30, 32], the starting point of investigations are different, resulting in different values of reduction factors for the same systems. The utilization of HV cables is new in the Turkish system and not very much is known on the effects of the cables. Further, the grounding of shielding and armoring wires is removed during the initial acceptance tests of grounding resistance. Therefore, they are assumed to be infinity. However, ground fault can only take place when the system is energized and under these circumstances, the cables supplying power are fully connected. In conventional designs, reduction factor is taken to be 0.65 and resultant fault currents are 35kA for 380kV systems and 20kA for 154kV systems.

The utilization of the computed per-unit overhead-line-earth-wire impedance between towers (\underline{Z}'_w) and the equivalent impedance (\underline{Z}'_p) are illustrated in the

system given in Figure 3.3. For this purpose, structure of a typical line-to-ground fault is drawn in Figure 3.3 and fault location is depicted by letter F.

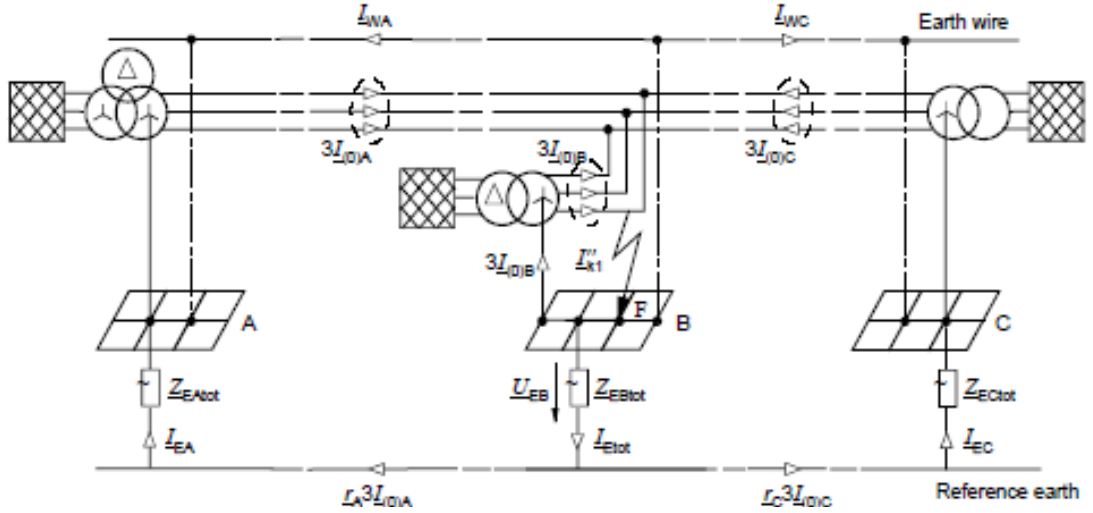


Figure 3.3: Line-to-ground fault case in a three station (A, B, C) system ([18])

It should be observed that total fault current, I_{Etot} , flowing through the grounding grid is smaller than line-to-ground fault current, I''_{k1} , because of the parallel overhead line grounding wires (I_{WA} , I_{WC}). Surface potential of the grounding grid B is computed as

$$\underline{U}_{EB} = \underline{Z}_{EBtot} \cdot \underline{I}_{Etot} \quad (3-8)$$

Line-to-earth fault current (I''_{k1}) at the location F can be computed as three times the zero sequence current, thus,

$$\underline{I}''_k = 3\underline{I}_{(0)A} + 3\underline{I}_{(0)B} + 3\underline{I}_{(0)C} \quad (3-9)$$

The total current through earth at the short-circuit location F at station B remote from other stations to which it is connected is:

$$\underline{I}_{Etot} = \sum \underline{r} \cdot 3\underline{I}_{(0)} \quad (3-10)$$

By Kirchoff's current law, it is easy to see the relation of \underline{I}_{Etot} in Figure 3.3 that

$$\underline{I}_{Etot} = \underline{r}_A 3\underline{I}_{(0)A} + \underline{r}_C 3\underline{I}_{(0)C} \quad (3-11)$$

Then, from Eqs. (3-10) and (3-11),

$$3\underline{I}_{(0)B} = 0 \quad (3-12)$$

Factors \underline{r}_A and \underline{r}_C are as a result of the mutual impedance between earth wires and phase cables of the system. With the assumption of perfectly balanced system, reduction of mutual impedances (\underline{r}_A , \underline{r}_C) on fault current can be taken as equal:

$$\underline{r} = \underline{r}_A = \underline{r}_C \quad (3-13)$$

Then, the following equation is derived by Eqs. (3-9) and (3-12).

$$\underline{I}_{k1}'' = 3\underline{I}_{(0)A} + 3\underline{I}_{(0)C} \quad (3-14)$$

And finally, \underline{I}_{Etot} is derived from Eqs. (3-11), (3-13) and (3-14).

$$\underline{I}_{Etot} = \underline{r} \cdot \underline{I}_k'' \quad (3-15)$$

where \underline{r} is defined as reduction factor for overhead lines (because of mutual effect). \underline{r} can be expressed by the following equation [18].

$$\underline{r} = 1 - \frac{\underline{Z}'_{WL}}{\underline{Z}'_W} \quad (3-16)$$

where \underline{Z}'_W is the earth wire impedance per unit length and \underline{Z}'_{WL} is the mutual impedance per unit length between the earth wire and parallel line conductors. \underline{Z}'_{WL} can be computed as

$$\underline{Z}'_{WL} = \frac{\omega\mu_0}{8} + j\omega \frac{\mu_0}{2\pi} \left[\ln \frac{\delta}{d_{WL}} \right] \quad (3-17)$$

where δ is the equivalent earth penetration depth and d_{WL} is the geometric mean distance between the earth wire and the line conductors L1, L2, L3. For the single earth wire configuration d_{WL} is calculated as

$$d_{WL} = \sqrt[3]{d_{WL1} \cdot d_{WL2} \cdot d_{WL3}} \quad (3-18)$$

while for the double earth wire configuration formulation is

$$d_{WL} = \sqrt[6]{d_{1WL1} \cdot d_{1WL2} \cdot d_{1WL3} \cdot d_{2WL1} \cdot d_{2WL2} \cdot d_{2WL3}} \quad (3-19)$$

Therefore, one can determine the total earth current from Eq. (3-15). This total earth current is flowing through total ground impedance given in Figure 3.4. This current is distributed into grounding grid and transmission lines as (i) part going through the grounding grid resistance (R), (ii) part going through the overhead lines, and (iii) part going through the cables' armoring and shielding.

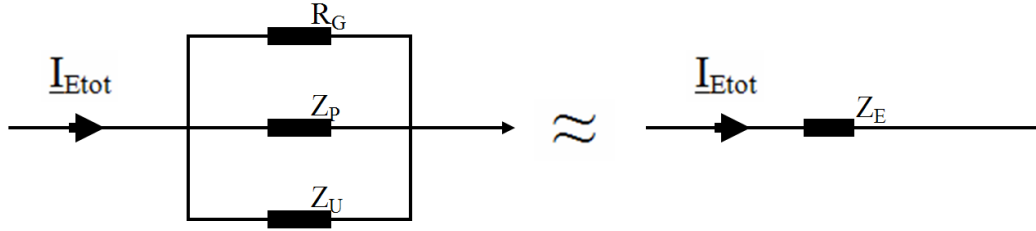


Figure 3.4: Total ground impedance

From Figure 3.4, the equivalent system grounding impedance, \underline{Z}_E , can be calculated as

$$\underline{Z}_E = \frac{1}{\frac{1}{R} + \sum \frac{1}{\underline{Z}_P} + \sum \frac{1}{\underline{Z}_U}} \quad (3-20)$$

From the current division, grid current, maximum-grid-current (I_G), is computed as

$$I_G = \underline{I}_{Etot} \cdot S_f \cdot D_f = \underline{I}_{Etot} \cdot \frac{\underline{Z}_P + \underline{Z}_U}{\underline{Z}_E} \cdot D_f \quad (3-21)$$

where S_f is the current division factor (which is acquired from current division in Figure 3.4) and D_f is the decrement factor [2].

3.3. Effects of Soil Treatment

Soil resistivity ([2], [16], [17]) is the primary material property that governs the grounding resistance. In a substation, soil resistivity varies between $10 \Omega \cdot m$ and $10000 \Omega \cdot m$. Since it is linearly related to the grounding resistance, researchers considered changing the soil characteristics of the substation as a part of the

design process. The collection of the methods developed to decrease the soil resistivity in a region is called the “soil treatment methods” in AC substation grounding.

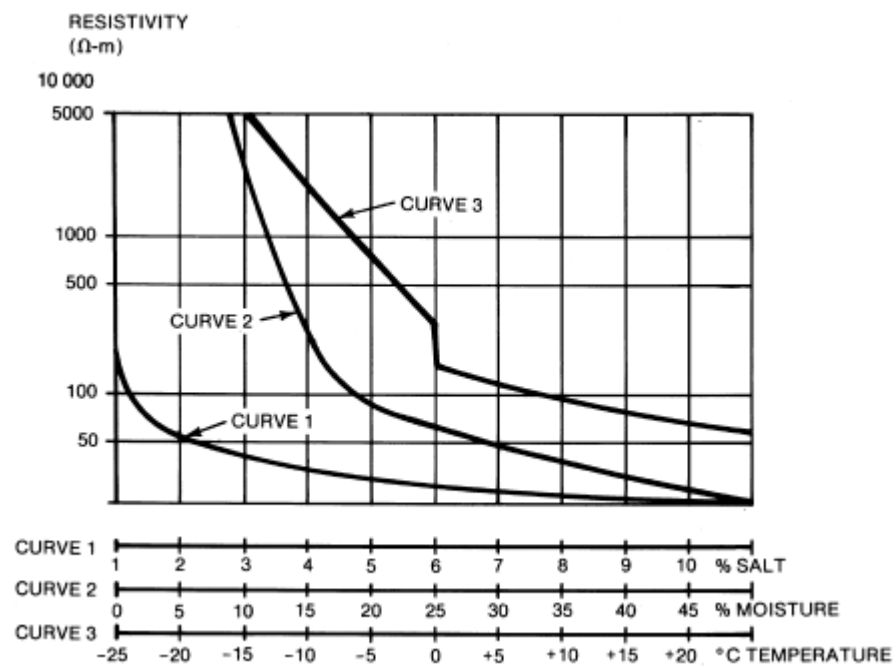


Figure 3.5: Effects of moisture, temperature, and chemical content on soil resistivity ([2])

Soil resistivity is highly dependent on the following three factors: moisture content, temperature and chemical content. For the first factor, the resistivity of most soils rise rapidly when the moisture content goes below 20 percent in weight. The second factor temperature has little effect on soil resistivity, except very low temperature cases. If temperature decreases to freezing levels, then resistivity increases rapidly. The final factor, chemical content, is inversely related with soil resistivity. This is because the typical chemicals (such as salt) in soil are

good ionizers. The change of soil resistivity with respect to these factors is given in Figure 3.5.

3.3.1. Soil Treatment by Addition of Electrolytes

An abundance of water does not necessarily result in higher resistivity. In areas where the soil is continually saturated, the soil resistivity may be high. This is due to the removal of electrolytic materials in the soil by prolonged leaching. Soil without electrolytes is a poor conductor. A range of soluble substances which add electrolytes to the soil such as salt (Sodium chloride), washing soda (sodium carbonate), epsom salts (magnesium sulphate), have been tried and tests generally show a vast reduction in soil resistivity with each. Unfortunately, the improvements are only short lived, since the salts become increasingly diluted in time. The durability, and hence effectiveness, of this method has been enhanced dramatically with application of calcium sulphate (gypsum). This material has low solubility but provides adequate conductivity.

3.3.2. Soil Treatment by Improving Moisture Retention

In soils which are extremely well drained or suffer prolonged periods of drought, the soil at earth conductor level may become extremely dry. If the moisture drops below 20% the resistivity of the soil increases exponentially. Adding material to the soil in the vicinity of the conductor prevents excessive moisture loss and keeps the resistivity within acceptable levels locally. Bentonite is such a material that hydrates chemically while holding water in its structure—Bentonite will absorb about five times its own weight in water. Also it can be used solely as a backfill material for grounding rod beds. It can also be mixed with soil with descent results. On the other hand, Bentonite is not capable of holding water indefinitely. If there is no moisture available in region, it will eventually dry out and shrink.

3.3.3. Soil Treatment by Improving the Contact Surface of the Electrodes

Although the material and moisture of the native soil may suggest low resistivity levels, a particular stony soil may cause a problem due to the lack of electrode versus soil contact. This contact can be improved by backfilling around the conductor with a suitable fine loam type soil which is cheap to obtain and can have low resistivity. Bentonite and conductive concrete Marconite may also be used as filling material. As mentioned, Bentonite will dry out in time, reducing its effectiveness. Marconite fills any void in the soil and is a durable solution.

Although these methods are used in practice, there is not any conventional formulation that predicts their effect. The current predictions are based on raw experience, or the finite element analysis. The finite element analysis test tool CYMGRD is capable of computing effects of contact surface materials (backfill materials) around rods.

3.4. Effects of Rods and Deep-Driven Rods

There are three purposes of using grounding rods in a system grounding design. First one is reaching to the lower earth layers, which are less affected by environmental factors such as temperature and moisture content. Second advantage is protecting the system operation as rods are sited near surge arresters as close as possible to minimize the effectiveness of transient voltages. Third is grounding the fences of the grounding region separately [16].

Earth rods are made of solid copper, stainless steel or copper bonded steel. Their typically 10-25mm in diameter and 2.5-3m long. The effective volume for each rod is a hemisphere with a radius of 1.1 times the rod length [17]. Hence, the distance between the rods should be at least 2.2 times the rod length; otherwise

destructive interference (defined as mutual effect) between the rods take place. For higher tolerance against the variation in weather conditions, the height of the rods is increased to 5m [17]. The effect of the rods on the grounding resistance can be computed via international standards and rod usage can be useful in the design process. They are not as effective in decreasing the ground resistance as the other methods though, and they are relatively expensive. Hence, in practice, rods are included in the design in minimal numbers mainly for the second and third purposes given above.

Some researchers investigated the effect of rods on the grounding resistance when their length is increased to 20-80 m. These types of rods are called “deep driven rods”. According to [19], the ground resistance of a deep driven rod is dependent on the number of earth layers, layer heights and layer resistivity. Figure 3.6 illustrate the multilayer structure of earth.

In Figure 3.7, the percentage decrease of earth resistance ($\zeta\%$) versus rod length divided by equivalent radius of horizontal grid (L/r_{eq}) is given [20]. The plot considers a two layer model with a grid size of 100 m x 100 m, upper layer resistivity, ρ_2 , of $200\Omega\cdot\text{m}$ and 40 m rod height. k is the reflection factor given by

$$k = (\rho_2 - \rho_1) / (\rho_2 + \rho_1) \quad (3-22)$$

where ρ_1 is the resistivity of the lower layer.

As shown in the graph, more negative k values lead to higher values in percentage decrease of earth resistance, or equivalently, more decrease in the resultant resistance of the grounding. Therefore, via Eq. (3-22), as the lower-layer resistivity becomes smaller, the effectiveness of the deep driven rods increases.

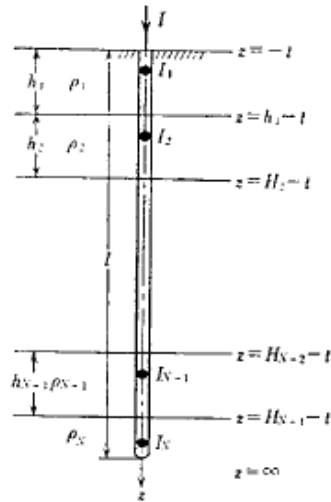


Figure 3.6: Multilayer earth structure ([19])

For multilayer cases, reference [19] includes a formulation to calculate the ground resistance. On the other hand, widely-used programs (e.g., CYMGRD, ETAP) that simulate ground grids are not yet capable of multilayer design—at most they can do two layer models. Obviously then, the rods in a multilayer case cannot also be modeled with these software. The primary reason that these codes do not consider the multilayer case is that, in reality, it is practically impossible to measure explicit layer thicknesses and their resistivities. Hence, such calculations are merely theoretical exercises. The practical problem is to find the equivalent two layer system which has the same ground resistance.

[26] is also noted at this point which compares uniform, two-layer and multilayer models with each other and experimental results. Quoting, they conclude that “Multilayer soils appear to behave like uniform or two layer soils derived from the multilayer soils by combining (averaging) the resistivities of adjoining layers which are not in contact with the grid.” Explicitly for the two layer model, lower layer represents the combination of lower levels in the multilayer design.

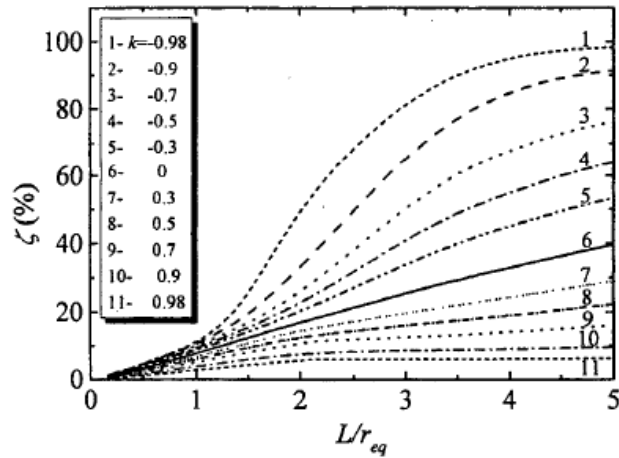


Figure 3.7: Relationship between the grounding resistance decreasing role of rods in the two-layer soil ([20])

Ultimately though, the actual effect of the deep driven rods can only be determined experimentally after the installation.

3.5. Explosion Method

Explosion method is developed by the researchers Meng and He [15] for grounding in regions with very high resistivity soil. Its first stage is drilling deep holes into the earth at the corners of the area to be grounded. Following this, explosives (e.g., dynamites) are placed in these deep-driven holes. Triggering the explosives result in many cracks that branch into the soil as shown in Figure 3.8. These cracks are then filled with low resistivity materials (grounding enhancement materials) with the utilization of high pressure pumps. Thus, a tree structure of low-resistivity material is formed under the grounding region. In the final stage, the top of the trees are connected to the grounding grid. The resulting structure of tree shaped electrodes is given in Figure 3.8.

Physically, this method replaces the planar electrode configuration with an approximate spherical electrode configuration. For the former, the ground resistance of a circular metallic plate or a dense grounding grid design of radius r can be approximated as [2]

$$R = \frac{\rho}{4r} \quad (3-23)$$

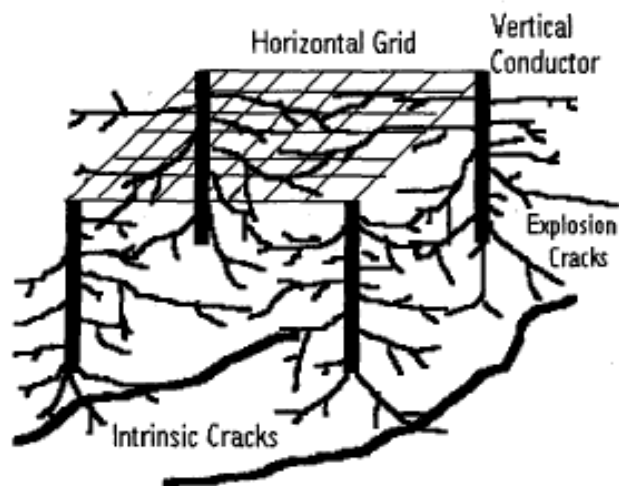


Figure 3.8: The explosion method: deep driven tree like electrodes connected to the grounding grid ([15])

For the latter (the case in Figure 3.8), the ground resistance of a hemispherical electrode of radius r is approximately given by

$$R_h = \frac{\rho}{2\pi r} \quad (3-24)$$

The difference between the ground resistances of a dense grounding grid and a hemispherical electrode can be computed as

$$DifferencePercentage = \frac{R - R_h}{R} \times 100 = R \left(1 - \frac{2}{\pi} \right) \times 100 \quad (3-25)$$

It follows from Eq. (3-25) that there is a 36.3% reduction in the ground resistance using a hemispherical electrode instead of circular plate electrode with the same radius. When the radius of the hemispherical electrode is increased to a value such as 1.5r, the grounding resistance is decreased by 57.5% which is considerable.

Reference [15] cites to such cases, in one, a substation with an area of 120m x 120m, the resistance has been calculated for a two layer soil model as 3.2Ω and has been reduced to 0.45Ω by the effect of explosion method. While in the second case, a ground resistance of 2Ω has been reduced to 0.35Ω.

Table 3.1: Geological factor table of explosion method ([15])

Geological Condition	Underground Layer with low resistivity	Explosion and Geology Factor K
Heavy Weathering	No	1,25 - 2,00
	Yes	1,67 - 3,33
Medium Weathering	No	1,00 - 1,25
	Yes	1,25 - 2,00
Light Weathering	No	0,77 - 1,00
	Yes	1,00 - 1,43

The empirical formula that is defined by [15] is given:

$$R = \frac{\rho}{2\pi r K_j} \quad (3-26)$$

where K_j is the geological factor and chosen from Table 3.1 according to weathering type and lower layer soil type.

3.6. Parallel Grid Method

When the standard procedures do not apply, there are some rather interesting solutions for high-soil resistivity system-grounding. One such design is the parallel grid construction where two separate grounding grids is utilized. This method is problematic though, since two grids that are at a relatively small distance to each other develop mutual impedance that impairs the benefit. The distance at which mutual impedance ceases to be a problem is called the separation distance. There is not an established formulation to determine the separation distance and this method is not included in the standards. However, effect of separation distance in a parallel grounding grid system can be studied by FEM analysis. Related analysis is given in section “4.4.a- Effect of Parallel Grid”.

CHAPTER 4

NUMERICAL STUDIES AND SIMULATIONS

4.1. Introduction

In CHAPTER 2, conventional grounding systems are analyzed, while CHAPTER 3 gives the methods and techniques that can be utilized in order to reduce the effective grounding resistance. In this chapter, the effectiveness of the revised methods will be discussed and found out through numerical calculations for different system parameters. The results obtained are composed with usage of the FEM analysis, and deviations are observed. Actual problems are considered and solved in multiple ways (including methods given in CHAPTER 3) to investigate effectiveness of results.

4.2. One Rod Grounding

It is shown in section “2.1.1.a- One rod grounding design methods” that there are three different formulations of grounding with one rod. A grounding problem is considered to compare these methods with the results taken from FEM analysis. Following data are given for determination of ground resistance.

- Resistivity of earth is given as 5 to 10 $\Omega \cdot m$.
- Rod length (L) is taken between 244cm and 350cm.
- Rod radius (d) is taken between 1.9 cm and 5 cm.

According to the results given in Table 4.1, Method II and Method III give very close results to each other and to FEM analysis. Maximum error between them never exceeds %5 percent compared to FEM for these two methods. On the contrary, error between FEM analysis and Method I is about %10 percent. Moreover, this method is more dependant on changes of rod diameter. Increased diameter of rod affect the ground resistance hugely compared to other two methods and FEM.

Table 4.1: One rod grounding solutions

ρ ($\Omega\cdot\text{m}$)	L (cm)	d (cm)	r (cm)	Method I R (Ω)	Method II R (Ω)	Method III R (Ω)	FEM R (Ω)
10	250	1,9	0,95	3,96	3,79	3,79	3,86
10	350	1,9	0,95	2,99	2,86	2,86	2,75
10	250	2,5	1,25	3,01	3,62	3,62	3,42
10	350	2,5	1,25	2,27	2,74	2,74	2,62
10	250	5	2,5	1,50	3,18	3,18	2,99
10	350	5	2,5	1,14	2,42	2,42	2,31
50	250	1,9	0,95	19,79	18,97	18,96	18,00
50	350	1,9	0,95	14,94	14,31	14,31	13,70
50	250	2,5	1,25	15,04	18,09	18,09	17,10
50	350	2,5	1,25	11,36	13,69	13,69	13,10
50	250	5	2,5	7,52	15,89	15,89	15,00
50	350	5	2,5	5,68	12,11	12,11	11,50

Results in Table 4.1, indicate that in the order of 10 $\Omega\cdot\text{m}$ soil resistivity, it is possible to keep resistance-to-ground in the region of 1 to 5 Ω which is fair enough for low voltage system grounding. However, in AC substation grounding GPR and touch voltage levels have to be checked. For 20kA —High Voltage Fault current— case, it is impossible to keep touch and step potentials in their safety limitations. In Figure 4.1, potential distributions of one rod grounding for 20kA case are given.

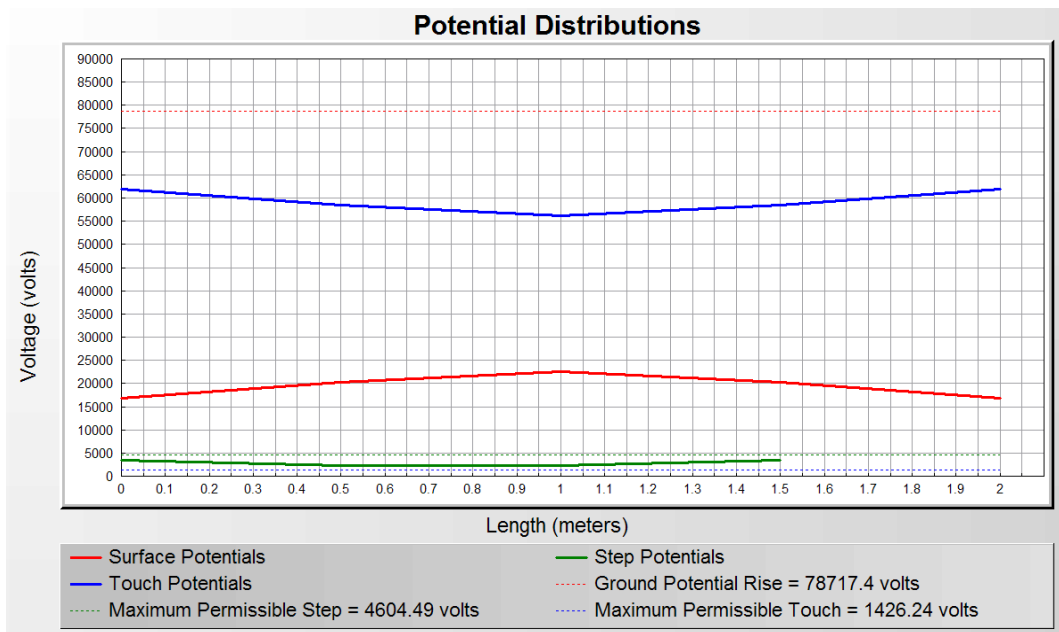


Figure 4.1: Potential distributions of one rod grounding

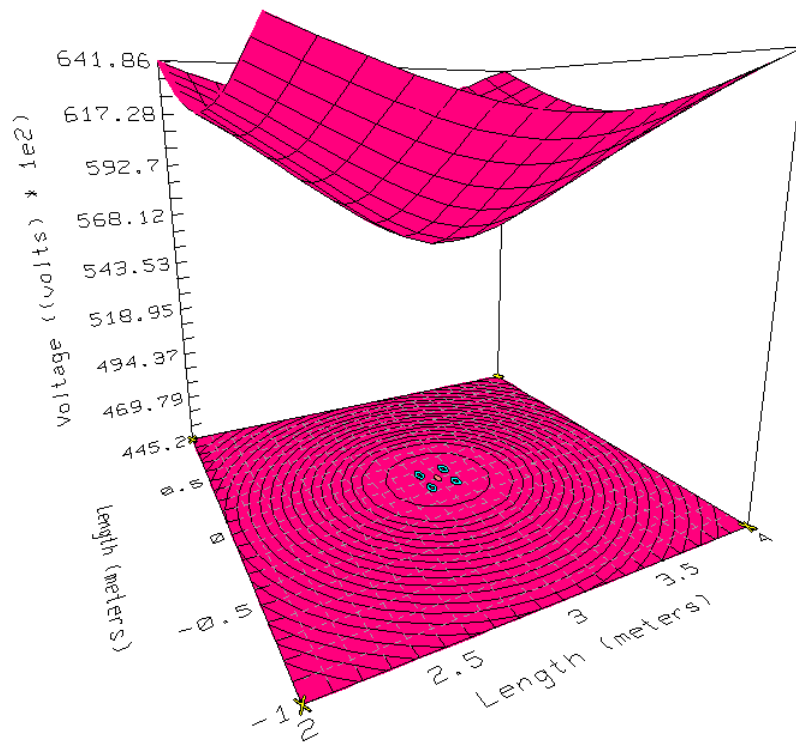


Figure 4.2: Touch potential for one rod grounding

Touch potential distribution of a one rod grounding system is simulated in Figure 4.2. In this simulation following data are used:

- Fault current: 20000A
- Rod Length: 2.5m
- Rod buried: 0.5 meter below the ground
- 50kg man weight

GPR is computed [2] from CYMRD simulation and its value is 78717 Volts. Maximum permissible touch voltage is computed and is found as 1426 Volts. As indicated in Figure 4.2, touch voltages are varying between 64186 Volts and 44520 Volts from 2 meters distance to the rod. GPR is enormously bigger than 20kV levels. Both GPR limitation and touch voltage criteria are unsatisfactory and are far from their maximum limits. So this kind of design is not applicable to HV and EHV AC substations. However, this kind of grounding can be used for LV systems where fault current and its duration are much smaller.

4.3. Mesh Systems

In this title, conventional grounding methods (given in CHAPTER 2), which include grounding grid design, will be analyzed and compared. Further, actual design problems are solved by different methods (including the methods in CHAPTER 3) in order to make an observation on them. In each problem, grounding parameters (grounding resistance (R), GPR, touch voltage and step voltage values) are checked and validity of the design is observed. In the first actual problem, problem is solved for both uniform soil model and two layer soil model. In addition, effect of division factor calculation is observed. In the second actual problem, design procedure is more problematic. Station area is very low and soil resistivity determination is more problematic. By using two layer soil model, a solution is built while observing effects of rods, deep driven rods, soil treatment and determination of fault factors in the design.

4.3.1. Comparison of Uniform Soil Model Methods

In CHAPTER 2 four conventional uniform soil modeling methods are given to compute ground resistance (R). All these methods are empirical and their results differ from each other according to the shape of grounding grids. Here, the resultant resistances of these methods are compared for different kind of grounding regions and shapes. In addition, CYMGRD program is used to compute ground resistance values for the same configurations. In CYMGRD manual, it is written that grid designs made in CYMGRD are dimensionless because of the nature of FEM analysis. So effectiveness of all conventional methods is compared according to the error calculated from the difference between FEM results and their results.

Assume a grid design problem to compute ground resistance of regions in different shapes and sizes with the following given data:

Uniform soil model resistivity: $100\Omega\cdot\text{m}$

Grid depth: 0.5m

Radius of grid conductors: 7mm

Changing Variables: Grid size (from 400m^2 to 4000m^2), number of meshes (16 to 40)

Table 4.2 includes computed resistances and their errors for uniform soil model. Results given in Table 4.2 are computed by a java program that is developed by the author to compare these conventional methods. Sample grid sizes and meshes which are used for simulations are chosen as close as possible to actual designs. For this purpose, grid sizes are taken to be between 400m^2 and 4000m^2 . The parameters a, b, c and d are taken as described by Figure 2.1 in section “2.1.1.d-IV. Thapar-Gerez Method”. Although many grid designs considered, less number

of grids and solutions are given in Table 4.2 to give an idea about results that are used to derive following assumptions by the author.

Table 4.2: Resistance calculation results in uniform soil models

	Grid Size a x b x c x d	Number of Meshes	Laurent Niemann Method		Sverak method		Schwarz Method		Thapar- Gerez method		CYMGRD FEM
			R	% Error	R	% Error	R	% Error	R	% Error	R
SQUARE SHAPE	20 x 20m	16	2,71	14,83	2,62	11,02	2,49	5,51	2,46	4,24	2,36
	40 x 40m	16	1,36	9,68	1,34	8,06	1,29	4,03	1,25	0,81	1,24
RECTAN- GULAR SHAPE	30 x 120m	16	0,98	25,64	0,89	14,1	0,76	-2,56	0,79	1,28	0,78
	20m x 80m	16	1,4	23,89	1,47	30,09	1,14	0,88	1,3	15,04	1,13
TRIANG- ULAR SHAPE	30 x100m	16	1,03	-3,74	0,91	-14,9	0,88	-17,7	0,78	-27,1	1,07
	60 x 200m	16	0,7	22,81	0,64	12,28	0,57	0	0,51	-10,5	0,57
L SHAPE	30 x 50 x 70 x 10m	16	1,09	36,25	1,03	28,75	0,99	23,75	0,83	3,75	0,8
	40 x 60 x 60 x 10m	16	0,88	20,55	0,87	19,18	0,85	16,44	0,73	0	0,73
T SHAPE	20 x 40 x 60 x 20m	32	0,85	14,86	0,9	21,62	0,89	20,27	0,73	-1,35	0,74
	40 x 60 x 100 x 20m	40	0,69	9,52	0,79	25,4	0,79	25,4	0,62	-1,59	0,63

All methods are giving close results in the case of square shape regions. However, in grids with sizes about 400m², results of Laurent Niemann and Sverak methods have errors about %15 percent. On the other hand, square grids having sizes

bigger than 1000m^2 , Laurent Niemann and Sverak methods have errors between %5 and %10. Further, Schwarz and Thapar-Gerez methods give results with errors about %5 percent or lower. In rectangular and triangular shaped grids, Laurent Niemann and Sverak methods have errors about %15 percent or higher. Thapar-Gerez method results mostly under %15 percent error. On the contrary, Schwarz method give results lower than %5 percent error. For L shaped grids, Laurent Niemann, Sverak and Schwarz methods have errors higher than %15 percent while, Thapar-Gerez method has very low percent of errors about % 5 percent. Last, in T shaped grids, situation is the same as L shaped grids. Again, Thapar-Gerez method has minimum errors in the region of % 5 percent.

Therefore, one can conclude the following results by considering above derivations. Although, Laurent Niemann and Sverak methods are applicable to the square shaped grids, which have over 1000m^2 area for the calculation of ground resistance, it is better to use Schwarz and Thapar-Gerez methods also in square shaped grids since they do not have an area limitation for accuracy. Laurent Niemann and Sverak methods are not good enough to apply in rectangular shaped grids since other methods Schwarz and Thapar-Gerez have percent errors less than %10 percent error, whereas Laurent Niemann and Sverak methods have errors higher than %15 percent. Schwarz method has less percentage of errors in both L, square and rectangular shaped conditions, but this is not the case for other shapes. In the case of triangular and T shaped grids Laurent Niemann, Sverak and Schwarz methods have over %20 percent of errors. At last, Thapar-Gerez method has still accurate enough error percentages in triangular, L and T shaped conditions.

As a result, while designing a grounding grid in uniform soil conditions, Thapar-Gerez method should be used with its accurate results compared to the finite element modeled and calculated results of conventional methods. If the grid structure is L-shaped, square or rectangle, Schwarz method can be used too.

4.3.2. Actual Design Problem 1

This problem is given to investigate differences between soil models. As it is known, uniform soil model is used to model earth structure as one layer in infinite thickness. In practice, this is not the case. From geological perspective earth is formed from number of different layers, so their soil characteristics differ from each other. To investigate this difference, in this problem, an actual GIS grounding situation is chosen with sensible (close measurement values) Wenner-four-pin test results. Area of the region is limited, but resistivity of soil measurements is not so high. Other necessary data are given:

- Maximum fault current in 154kV System = 31,5 kA
- Fault Current Through the mat = 20 kA (r is taken as 0.65)
- Minimum area of conductor = 120 mm² (minimum)
- Rod diameter (d) = 2,5 cm
- Rod Length (L) = 250 cm (minimum)
- Depth of conductors (h) = 50 cm (minimum)
- Step length = 1 m
- Fault Duration (t_s) = 0,5 s
- Human impedance = 1000 Ω
- Surface layer resistivity (Crushed rock) = 2500 $\Omega.m$ (maximum)
- Surface layer height = 15 cm
- 74m x 50m Gird size
- One over head line connected to station
- Resistivity values which are acquired from Wenner-four-pin test results are given in Table 4.3. A, B, C are different horizontal paths in the region and D is the vertical path in the center of the region.

Table 4.3: Wenner test results for uniform soil problem

a (m)	A	B	C	D	AVERAGE
2	127	209	179	191	176,5
4	138	241	185	204	192
6	118	236	128	161	160,75
8	120	242	133	145	160
10	122	242	129	165	164,5
12	129	121	95	160	126,25
14	133	183	130	140	146,5
16	152	184	120	172	157
18	149	166	148	-	154,33
20	151	175	103	-	143
22	169	206	115	-	163,33
24	154	222	103	-	159,67
26	158	152	112	-	140,67
28	156	170	131	-	152,33
30	160	199	92	-	150,33
32	177	230	160	-	189
					158,51

Two separate solutions are given here. Solution 1 includes a designed grid in a uniform soil model composed of rods and grid conductors given in Turkish standards. First grounding parameters are observed without overhead line effect (current division factor) on the design. Then, this effect is considered and parameters are recalculated. The enhancement of the design is observed. Solution 2 includes the same grid configuration except the soil model. In this case, two layer soil model is used and grounding parameters are observed and compared with Solution 1.

Desired design solutions must have GPR around 20kV and R value around 1 Ω according to National Grounding Design Standards [21] with step & touch voltages in safe margin according to [2].

a- Solution 1

In order to obtain uniform soil model, Wenner-four-pin test results have to be considered. A graph that is composed of average resistivity values obtained from different electrode spacings is drawn to calculate approximate soil resistivity and it is given in Figure 4.3.

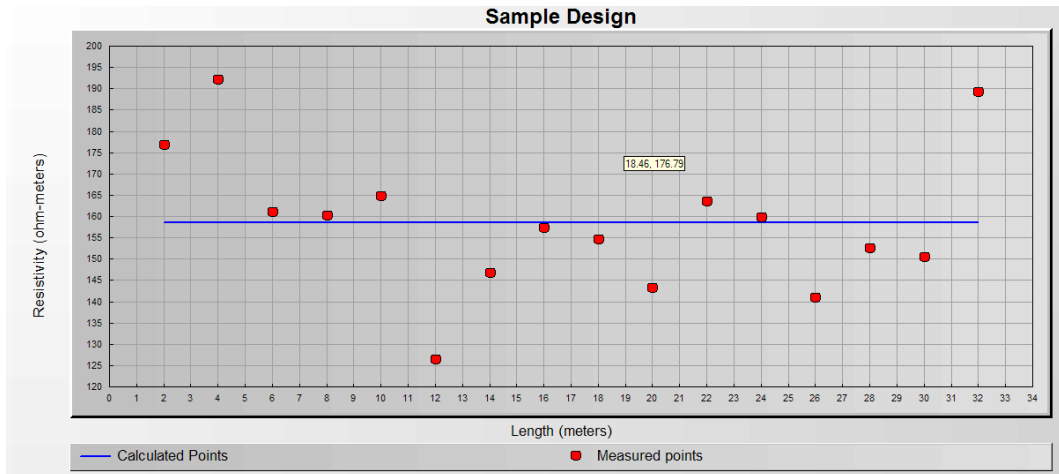


Figure 4.3: Sample design soil resistivity determination

Since all the results close to each other, taking the average value of all results for different electrode spacings can be used to determine the soil resistivity as it is given in Table 4.3. Uniform soil resistivity value is computed as $158,51\Omega$ and in Figure 4.3, this average value is drawn as a line.

An initial grid configuration is designed by the author and it is given in Figure 4.4. There are 76 rods in this design and total length of grid conductors used in design is 2508m. With the given grid configuration, Thapar-Gerez method (discussed in section 2.1.1.d-IV. Thapar-Gerez Method) ground resistance (R) is

determined to be 1.33Ω . On the other hand, FEM analysis compute ground resistance (R) to be 1.11Ω for the same grid design.

Ground potential rise ($GPR=R \cdot I_G$) of the given grid design is computed by ground resistance (1.11Ω) and grid current ($I_G = 20\text{kA}$). Moreover grid current is calculated by division factor ($S_f = 1$), reduction factor ($\underline{r} = 0.65$) and decrement factor ($D_f = 1.0313$). These values are chosen according to national standards [21] and none of them are computed explicitly for this specific problem. From these calculations, GPR is calculated to be 22973 Volts.

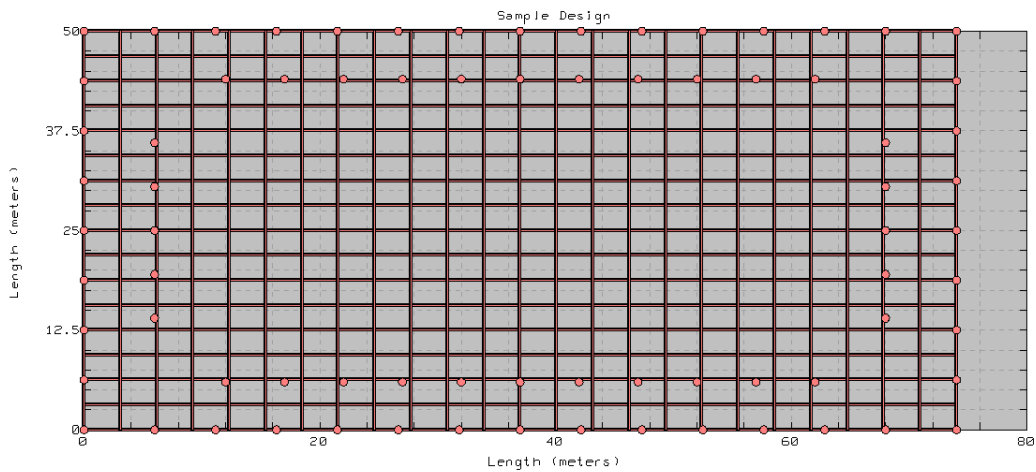


Figure 4.4: Sample grid design

Potential distributions from left-bottom corner to right-upper corner are given in Figure 4.5.

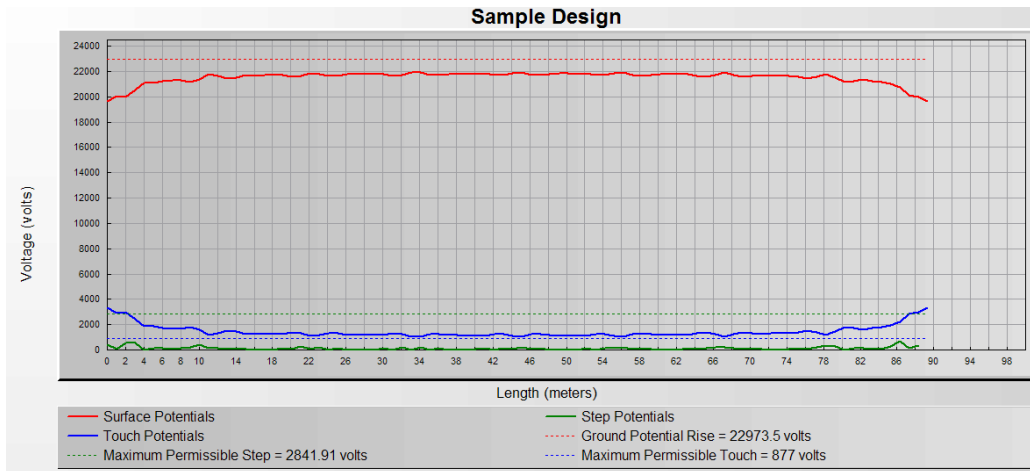


Figure 4.5: Potential distributions of sample design

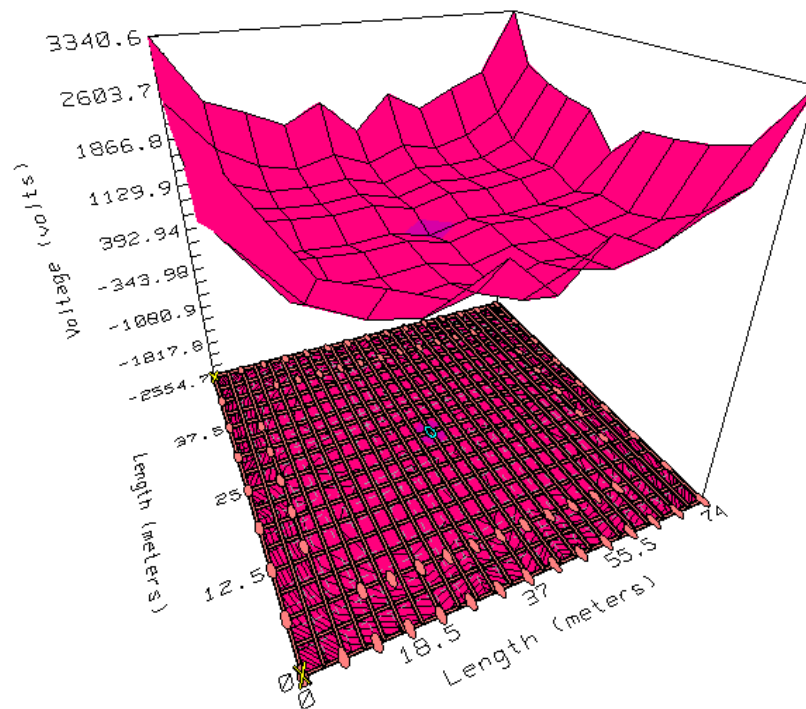


Figure 4.6: Touch potential distribution of sample design

Maximum permissible touch potential is calculated as 877 Volts and Figure 4.5 shows the touch, step and surface potential distributions along the grounded area.

In Figure 4.5, step potential distribution is always under maximum permissible step potential (2841 Volts). On the other hand, touch potential in the region is not safe because value of touch potential is bigger than maximum permissible touch potential for most of the points. In Figure 4.6, touch potential distribution is given in three dimensional view. In this figure, all regions are in the danger of high touch potential. Therefore, it can be observed that the design has to be enhanced. For the enhancement of design, division factor is recalculated for this special substation configuration without omitting overhead line impedance.

For this purpose, first, overhead line earth wire impedance (Z_w) between two towers is calculated as 0.295Ω according to the Eq. (3-5). Second, the equivalent earth wire impedance of one line is computed from Eq. (3-1) as 2.52Ω . There are no connected cables to the system so cable shielding and armoring impedance is taken as infinite. From Eq. (3-20), equivalent impedance of the system is computed as 0.77Ω . Current division factor (S_f) is found as 0.717 by Eq. (3-21) and I_G is determined as 14354A.

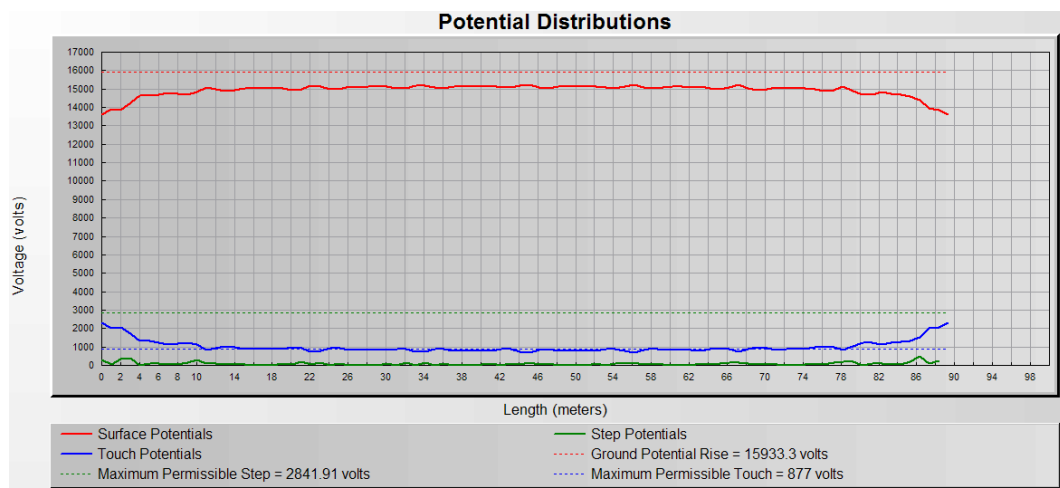


Figure 4.7: Potential distributions of sample design after z_e determination

For the same grid configuration, potential distribution graph is redrawn in Figure 4.7. As shown, touch potential and step potential voltage lines are lowered in magnitude and in most of the region, these potential are below their maximum permissible values. GPR value decreases from 22973 to 15933 Volts and is still bigger than surface potential. Further, touch voltage distribution is given in Figure 4.8 and touch potential is necessarily lowered across the region. Since all grounding parameters are satisfactory in their safe margins, this design is safe enough for installation and operation. As a result, determination of grid current without omitting overhead line effect protects the designer from using unnecessary additional grounding equipments as a design improvement. In all designs, division factor (S_f) has to be reconsidered and computed for that specific configuration in order to obtain satisfactory and economically feasible designs.

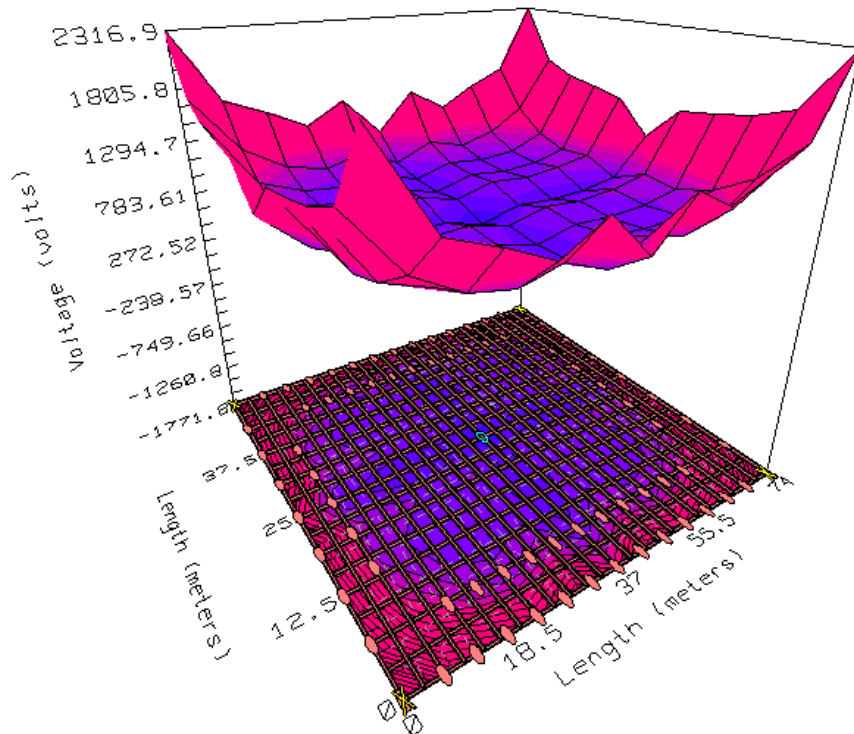


Figure 4.8: Touch potential distribution of sample design after z_e determination

b- Solution 2

In Solution 1, uniform soil model is made without omitting fault current determination. Here, the same design is simulated except soil model is two-layer in this case. For achieving a two layer soil model, Wenner-four-pin test results given in Table 4.3 have to be reconsidered. A best fitting function is computed from error minimization (discussed in section 2.1.1.e-I. Determination of an earth model by minimizing error function). This calculation is done using CYMGRD and a graph of soil resistivity is given in Figure 4.9. Following soil characteristics are obtained by calculations:

Upper Layer Resistivity = 188.57 $\Omega\cdot\text{m}$

Lower Layer Resistivity = 149.83 $\Omega\cdot\text{m}$

Upper Layer Thickness = 2.45 m

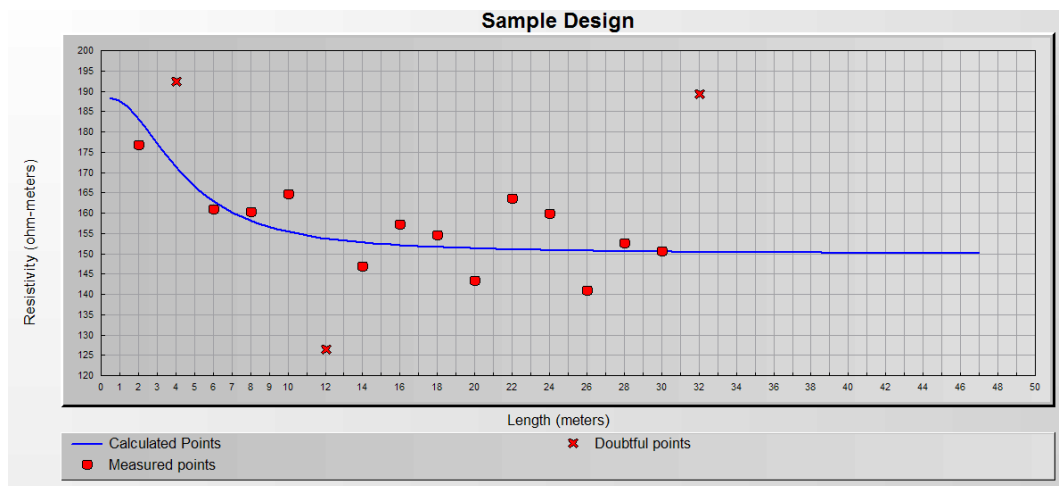


Figure 4.9: Soil layers resistivity determination

Two layer soil model is clearly defined. Then, for the same configuration of conductors and rods given in Solution 1, system is simulated by CYMGRD to

obtain grounding parameters for this case. Further, Sunde graphical method is tried but it is difficult to apply with test results given in Table 4.3 because it is hard to draw a resistivity graph as Figure 2.4 in this problem. In this situation, as a result, the graphical methods are not applicable for all cases. Calculated ground parameters are:

Ground Potential Rise is determined as 15728 volts.

Ground resistance (R) is 1.09Ω .

From new R value, Z_E is found as 0.76Ω with the effect of overhead lines (Z_P).

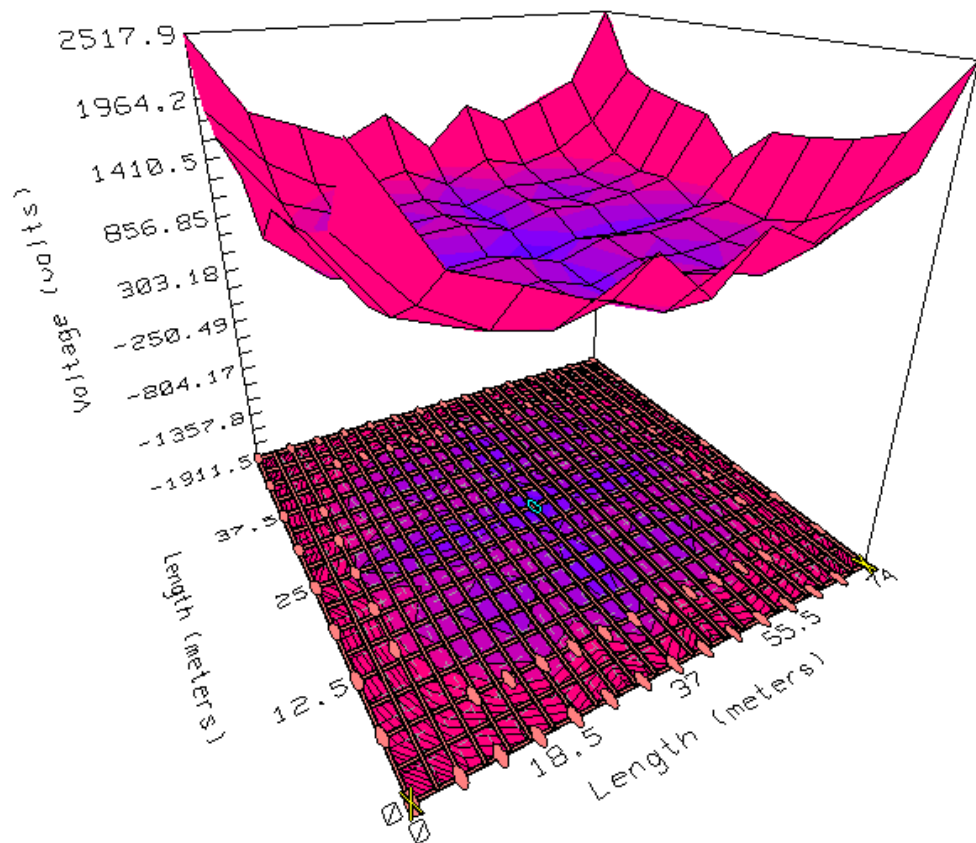


Figure 4.10: Touch potential distribution of sample design after z_e determination with two-layer model

Calculated grounding parameters (GPR, ground resistance and step voltage distribution and touch voltage distribution) are very close to uniform soil case. R differs from 1.13 to 1.09 and Z_E differs from 0.77 to 0.76. GPR almost does not change. Touch potential distribution shown in uniform soil model has slightly low values compared to two layer soil model given in Figure 4.10. Two layer soil model solutions are more reliable because it represents the earth model better. Potential distributions are given in Figure 4.11 to compare potentials given in Figure 4.7 for uniform soil model. From comparison, it is clear that potentials do not differ much from each other.

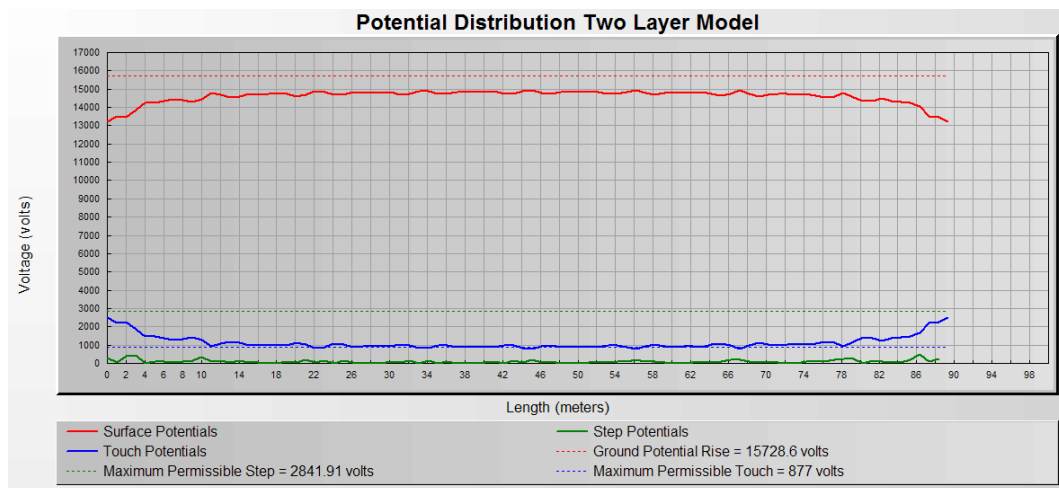


Figure 4.11: Potential distributions

According to these results, following derivations can be made. One can say that for measurements having close and low value resistivity, uniform soil model can match the results of two layer soil model. In other words, if Wenner-four-pin test results give close enough results in the range of 10-400 Ω , uniform soil model can be applied instead of two layer soil model. If there is a program present capable of designing the system in two layer soil model, of course it is better to model the

system in two-layer for best modeling geological structure of the grounding region.

4.3.3. Actual Design Problem 2

This problem is given to investigate problematic grounding design cases and observe the effectiveness of design improvements discussed in CHAPTER 3. Two-layer soil model will be used to determine soil characteristics in the solution. An actual GIS grounding situation is chosen with Wenner-four-pin test results taken in different time intervals. Region to be grounded is not only very limited in size, but also having hard soil characteristics. In more detail, resistivities taken from soil measurements are very high and inconsistent. Other necessary design data are submitted as:

- Maximum fault current in 154 kV System = 31,5 kA
- Fault Current Through the mat = 20 kA (r is taken as 0.65)
- Minimum area of conductor = 120 mm² (minimum)
- Rod diameter (d) = 2,5 cm
- Rod Length (L) = 250 cm (minimum)
- Depth of conductors (h) = 50 cm (minimum)
- Step length = 1 m
- Fault Duration (t_s) = 0,5 s
- Human impedance = 1000 Ω
- Surface layer resistivity (Crushed rock) = 2500 $\Omega.m$ (maximum)
- Surface layer height = 15 cm
- 86m x 50m grid size
- 2x154 kV overhead lines connected to station
- 27x34.5kV cables connected to system, no cables are connected while starting of station operation
- Resistivity values are read from Wenner –four-pin tests are given in Table 4.4.

Table 4.4: Wenner-four-pin test results

	TEST 1		TEST 2		TEST 3		TEST 4		TEST 5		TEST 6		TEST 7		TEST 8		TEST 9		TEST 10		
	R (Ω)	ρ ($\Omega.m$)	R (Ω)	ρ ($\Omega.m$)	R (Ω)	ρ ($\Omega.m$)	R (Ω)	ρ ($\Omega.m$)	R (Ω)	ρ ($\Omega.m$)	R (Ω)	ρ ($\Omega.m$)	R (Ω)	ρ ($\Omega.m$)	R (Ω)	ρ ($\Omega.m$)	R (Ω)	ρ ($\Omega.m$)	R (Ω)	ρ ($\Omega.m$)	
A																					
1	420	4402	81	853	36	377	50	524	57	597	410	4297									
2															24	327	126	1692	142	1902	
2,5	80	1311			96	1573	96	1573	104	1704	80	1311									
3			21	416	120	2330	117	2272	114	2214											
4									141	3605					4	89	76	1952	87	2218	
5			20	623					154	4892					5	148					
6	18	684	17	646					162	6154	18	684	7	247	6	228	52	1963	76	2882	
8	14	707									14	707	8	385	4	182	46	2343	70	3525	
10	10	630	14	895							10	630	8	530	2	146	45	2848	58	3660	
12	8	604	4	325							7	529	10	728	2	173			51	3878	
14													9	829	2	182			58	5107	
16													9	955	2	237			48	4855	
18													9	969	1	78			45	5124	
20													10	1300	1	72			41	5103	
22															2	310			31	4322	
24															2	253			26	3912	
26															3	418			23	3752	
28																			20	3541	
30																			10	1835	
32																			8	1512	
Average		1390		626		1427		1304		2839		1360		524		217		2159		3571	

Solution of this problem is divided into multiple parts to observe different method effects explicitly. In each part, grounding parameters are observed and effectiveness of methods are discussed in both accuracy and cost perspectives. In the first part, two-layer soil model parameters are determined and a grounding grid is designed. Then, in the second part, first enhancement is applied to design by increasing the number of rods. Third part includes addition of deep driven rods to grid design. Fourth part investigates effectiveness of the soil treatment in the soil around rods and deep-driven-rods. In the final part, reduction factor and current division factors are computed for this specific problem.

Desired design solution must have GPR around 20kV and resistance value around 1Ω according to National Grounding Design Standard [21] with acceptable step & touch voltages [2].

a- Part 1 Determination of Soil Characteristic and Design of a Sensible Grid

After various tests in the grounding region, Wenner-four-pin test results are obtained in different time intervals. Each test includes different set of resistivity values for the same electrode spacing. Determination of two-layer soil resistivities is more complex in this design. Two different approaches can be used for test result consideration. In the first one, average of resistivity values can be obtained with respect to different electrode spacings and error minimization can be used by these average values. This approach includes very high resistivity values, which are probably measured by mistake or electrodes that are surrounded with a rocky region, in averages, so the computed soil characteristic parameters get higher values than they should be. Another approach is that median of resistivity values measured with respect to different electrode spacings can be obtained as an input for error minimization. If sufficient number of tests is made on one electrode spacing, this method fits better for soil resistivity determination problems. Here,

there are ten different test results, so median method can give more reliable results.

List of average and median values are given in Table 4.5. By using median values given in Table 4.5, error minimization methods are applied to compute soil characteristics of earth in the region. Obtained soil resistivity characteristic curve is given in Figure 4.12, where points are the median resistivity values and “x” are the median values that have more than 10 percent error. Obtained earth characteristics are:

Upper layer thickness is 2.63 meters.

Upper layer resistivity is 1048 $\Omega\cdot\text{m}$.

Lower layer resistivity is 714 $\Omega\cdot\text{m}$.

Table 4.5: Configured test results as average and median values

a	AVERAGE		MEDIAN	
	R (Ω)	ρ ($\Omega\cdot\text{m}$)	R (Ω)	ρ ($\Omega\cdot\text{m}$)
1	101,00	777,10	101,00	777,10
1,5	175,73	1841,84	69,20	725,28
2	97,56	1306,79	126,29	1691,57
2,5	76,51	1253,64	88,00	1441,84
3	75,11	1458,60	114,00	2213,89
4	63,17	1615,09	76,35	1951,95
5	59,42	1887,33	19,60	622,58
6	44,38	1685,96	18,00	683,83
8	25,91	1308,05	14,00	706,78
10	21,17	1333,96	10,00	630,07
12	13,76	1039,49	7,50	566,58
14	23,15	2039,58	9,41	828,93
16	20,03	2015,50	9,49	955,08
18	18,17	2057,13	8,56	968,95
20	17,16	2158,32	10,34	1300,27
22	16,75	2316,00	16,75	2316,00
24	13,81	2082,76	13,81	2082,76
26	12,76	2085,37	12,76	2085,37
28	20,12	3540,96	20,12	3540,96
30	9,73	1834,63	9,73	1834,63
32	7,52	1512,40	7,52	1512,40

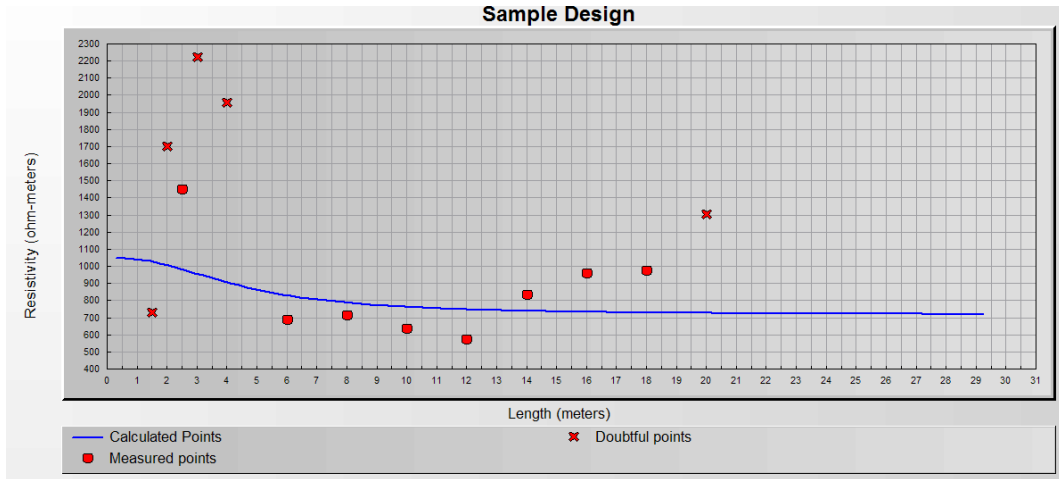


Figure 4.12: Soil resistivity characteristic curve in two-layer soil model

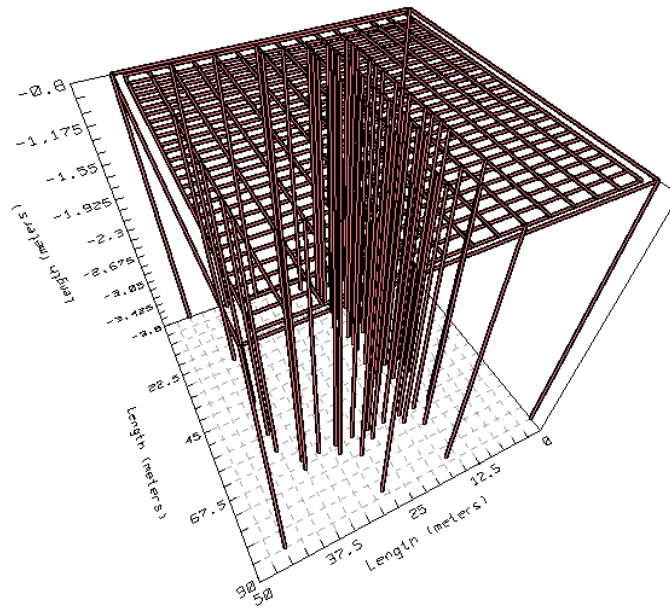


Figure 4.13: Structure of grid design without any enhancement

A sensible grid design is configured to simulate grounding parameters. This grid composes of 69 rods (that are 2.5m in length and 25.4mm in diameter [21]) and total length of used rods is 207m. In addition, 2674.5m of mat conductors are used in this design. Fence grounding conductors are 2m far from the main grid and four of the rods are used for fence grounding. Obtained grid structure is given in Figure 4.13.

Calculated ground resistance is 5.16Ω without including effect of over head lines and cables. Potential distributions are given in Figure 4.14. Grid current is taken as 20kA and GPR reaches to 106527kV, which is an unacceptable value for a grid design. Maximum permissible step and touch voltages are computed and their values are 10792Volts and 2864 Volts. Potential distributions from left bottom corner to right upper corner are given in Figure 4.14.

As shown in Figure 4.14, although step potential is in permissible values, touch potential distribution exceeds its maximum permissible value in the entire region. In addition, ground resistance is five times bigger than desired value of 1Ω which is unacceptable according to Turkish regulations.

As a consequence, excessive amount of conductors are used in the grid design (including mat conductors and rods) whereas most of the grounding parameters (R, GPR, touch voltages in grounding region) are far from a satisfactory design. Therefore, enhancement methods explained in CHAPTER 3 can be used to make necessary changes.

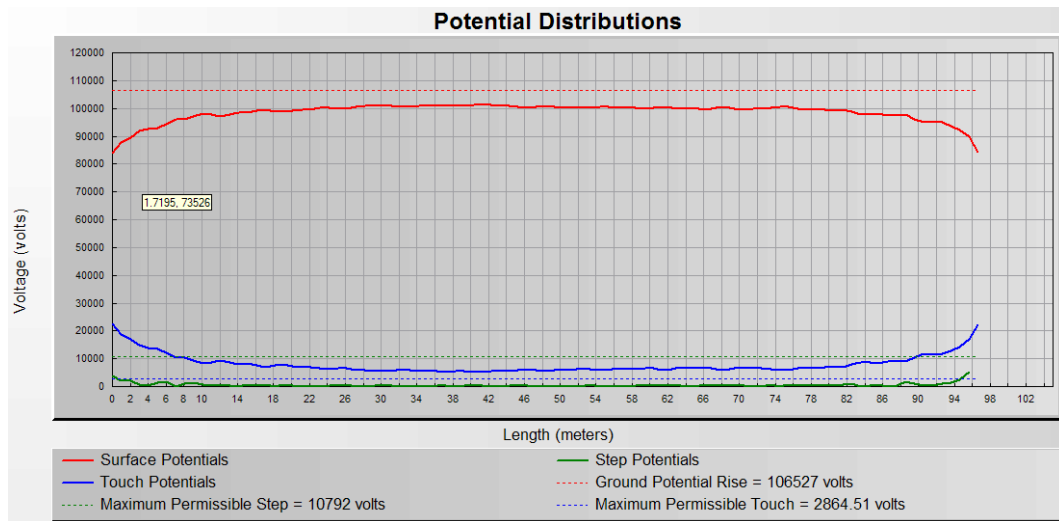


Figure 4.14: Potential distributions from left-bottom corner to right-upper corner

b- Part 2 Effect of Additional Rods

As a first approach, most of the time, field engineers try to use more rods in grounding systems to enhance the system. In order to investigate, if this is a true way to achieve satisfactory designs, number of rods in this system is varied. So far there are 69 rods placed in the system. In this title, increased number of rods effect is investigated by FEM analysis. In order to see this effect, 40 more rods are sited on the sides of grounding grid. Empty circles demonstrate rods sited in addition to the original grid, in Figure 4.15.

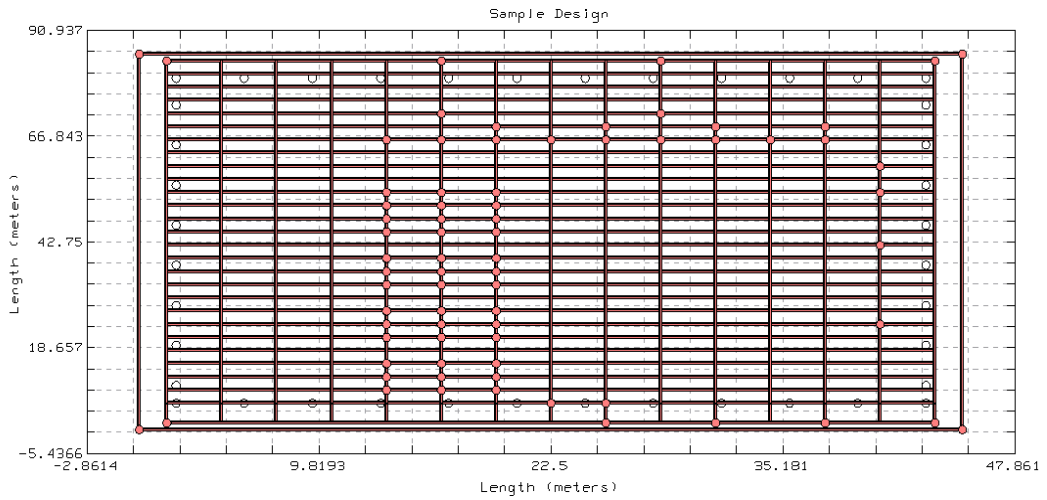


Figure 4.15: Grid design with additional 40 rods

After simulating the new system, calculated ground resistance (R) decreases to 5.12Ω . GPR slightly decreases to 105702 Volts. In order to observe results, touch and step potentials are given in Figure 4.16.

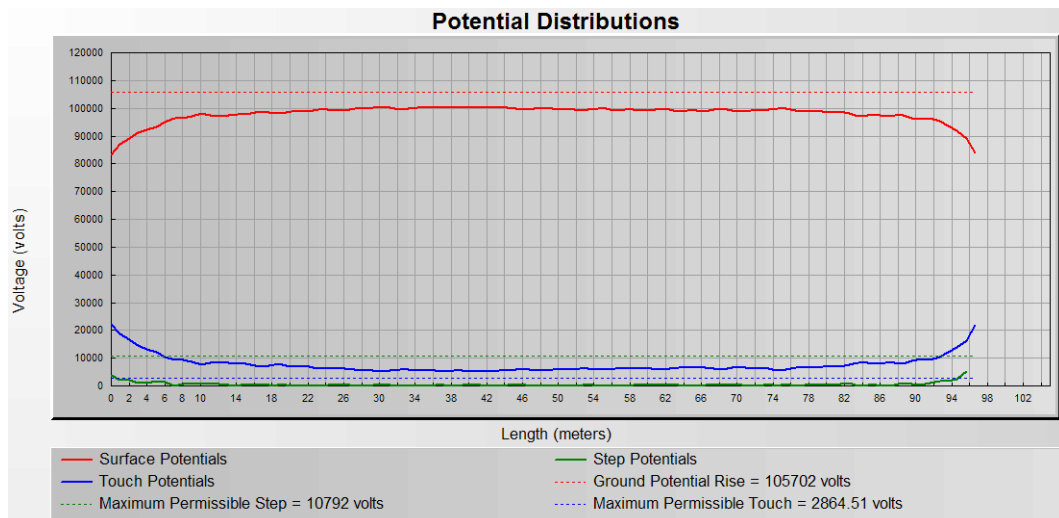


Figure 4.16: Potential distribution with additional 40 rods

As shown, touch potential distribution is still significantly higher than maximum permissible value and GPR is still so high. Moreover, placing 40 more rods almost have about %1 change on grid resistance R as in the calculation $(5.16-5.12)/5.16*100 \approx 1\%$. Resultant effect of additional rods is so small that is an interesting situation.

From the numerical analysis perspective, increasing number of rods only increases the length of conductors used. As it is mentioned above, there are (2674.5m + 207m) 2881.5m of conductors used in the design. Additional 40 rods means additional (40*2.5m) 100m of conductors. So the effect of adding rods is limited. Consequently, additional rods can not be considered as a cost effective way to decrease R value with its low R reduction in the order of 1-2 percent, especially in heavy grounding mat configurations.

c- Part 3 Effect of Deep-Driven-Rods

The main purpose of placing deep driven rods to the grounding grid is to reach the lower resistivity layers such as water sources under the ground. In order to effectively use this method, multilayer structure of earth has to be determined as detailed as possible. Researchers made many multilayer analysis and found some methods to determine multilayer structure. However, programs, which are present, cannot simulate multilayer earth structures. Two layer model is the only way to go on the solution. In two layered model, if sufficiently tall enough deep driven rods are used, lower layer resistivity of two layer model can simply add the minimum effect of lower resistivity layers of multilayer structure in the computations. For this purpose, deep driven rods are chosen as tall as possible whereas there are other parameters like mechanical structure and cost efficiency, which prevent the choice of longer deep driven rods. Rods can be drilled into about 100m

mechanically, but from the cost perspective, using deeper than 40m rods are not cost efficient.

For the explained reasons above 30m and 40m deep driven rods are used and their effectiveness are checked in a the two layer soil model by using FEM analysis.

The design is improved by placing four deep-driven-rods (that are 30m in length) at the corners of grounding grid (Figure 4.17). Then, ground resistance (R) and GPR values are recalculated. Ground resistance decreases to 4.50 Ω and GPR value decreases to 92965.2 volts. Although GPR value is still high, R significantly decreases about 13 percent from the given computation $(5.16-4.50)/5.16*100 = 12.7\%$.

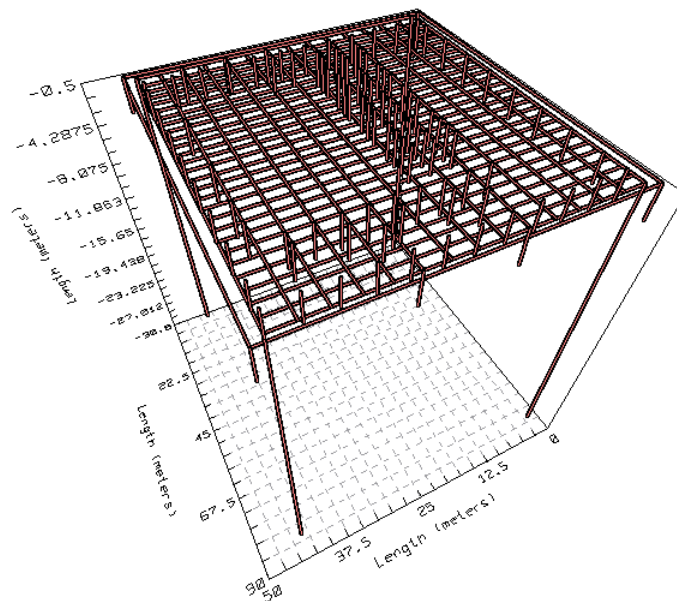


Figure 4.17: Grid design enhanced with 4 deep driven rods

Number of deep driven rods should not be increased since two rods must have a distance between each other about 2.2 times their length according to [17] in order to neglect their mutual impedance effect. Rods, which are 30m in length, are placed on the corners in a size of 86m x 50m grid. Rods that are separated 50m have mutual effects on them. On the other hand, rods that are separated 86m apart, do not have any available space for additional deep driven rods between them. So there is no more available space to place any additional deep driven rods. In fact, may be, length of rods can be increased.

Assume rod lengths are increased from 30m to 40m. In this case, calculated ground resistance (R) decreases to 4.23 Ω and GPR value decreases to 87371.4 volts. All four rods are changed and their length increased about 10m but change in the grounding resistance becomes about $(5.16-4.23)/5.16*100=18\%$. As it is observed, deeper rods give better decreases on R and GPR, but cost is increasing very rapidly with increased rod lengths.

In deep driven rods study, it is shown that deep driven rod effects on R and GPR is very much. Their effect is about 15-20% reduction in both R and GPR. However, potential distribution, which belongs to 30m deep driven rods case, given in Figure 4.18, is still not accurate enough. Still maximum permissible touch voltage values are lower than touch potentials. More design improvements are needed.

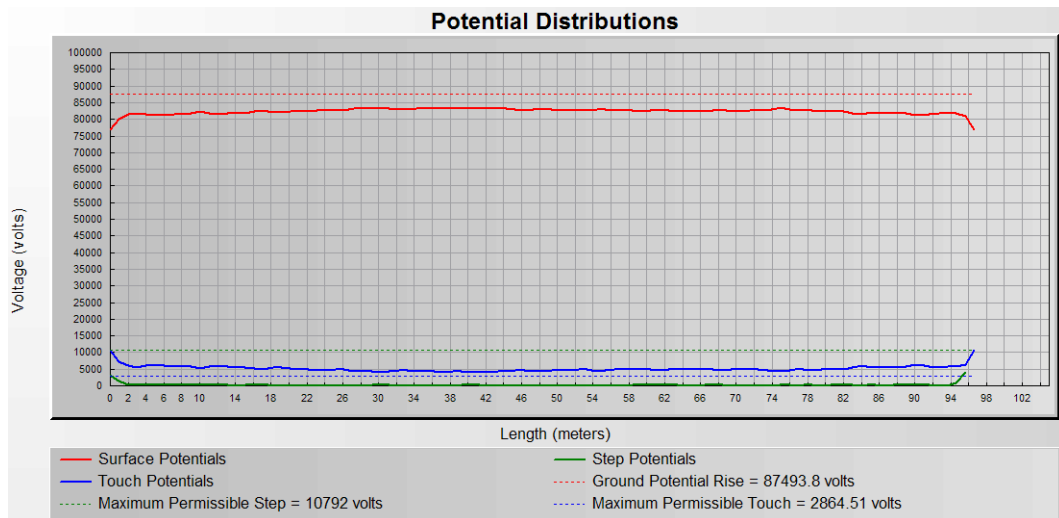


Figure 4.18: Potential distributions after addition of 4 deep driven rods

d- Part 4 Effect of Soil Treatment

Two kind of soil treatment can be applied to enhance this grounding design. First one is soil treatment for the entire region. Second one is replacing or treating the soil around rods to increase their effectiveness. Here second treatment method is analyzed. For the first method please refer to [17], [22], and [23].

There are 4 deep driven rods and 69 rods in this system. Three simulations are done by including enhancement material around these rods to investigate effects of this method.

In the first simulation $10\Omega\cdot\text{m}$ grounding enhancement material (GEM) is sited around deep driven rods with a thickness of 150mm. As simulated above 4.50 Ω is the R value after placement of 30m tall deep-driven-rods. Calculated ground resistance (R) decreases to 4.24 Ω . Effect of GEM can be computed as $(4.50 - 4.24)/4.50 \times 100 = 6\%$ on deep driven rods. A significant decrease is made with the combination of deep driven rods and GEM material around them. Combined

effect can be calculated as $(5.14-4.24)/5.14*100=17.5\%$. GPR value decreases to 87493 Volts, which is still so high.

In the second simulation, thickness of the GEM is increased to 300mm. Resultant R after simulation is 4.13 Ω . Decrement effect can be computed as $(5.14-4.13)/5.14*100=19.6\%$ with the combination of deep driven rods and 300mm width GEM. GPR value decreases to 85307 Volts. In this simulation GEM material usage is increased about 4 times (thickness is cylindrical) and the resistance gain of design is about $((4.24-4.13)/4.24*100) \%2.6$ compared to 150mm-width-GEM case. GEM usage around 150mm thickness is more cost effective compared to 300mm case.

In the third simulation, GEM usage around standard rods (2.5m length) is investigated. There are 69 rods in the grid design as mentioned above. Assume deep driven rods are present, but there is no GEM around them. For this case R value is 4.50 Ω as mentioned above. After the usage of 150mm GEM around rods, R is 4.47 Ω . Gain from the usage of GEM is computed as $(4.50-4.47)/4.50*100\approx 1\%$. This is an interesting result that cost of GEM usage is significantly increased, but decrease of R is almost negligible. Also, GPR value reduction is negligible.

After these simulations following decisions can be made:

- It is simply meaningless to use GEM around standard rods.
- Using GEM around deep-driven rods can be helpful to decrease R significantly about 6-8%.
- Using GEM with increased thickness does not do the desired effect on the reduction of R. There is an optimum value between 150mm and 300mm thickness of GEM.

GEM usage is a useful tool, but its effect is not large enough to satisfy the requirements of this problem. In this design, there are 69 rods (2.5m length, 25.4mm diameter), 4 deep driven rods (30m length and 25.4mm diameter), GEM (resistivity of $10\Omega\cdot\text{m}$, 150mm thickness) around deep driven rods in the design and resultant R is $4.24\ \Omega$ and GPR is 87493 Volts. GPR has to be around 20kV but it is far from desired value. Both touch and step criteria are not satisfied. Therefore, new improvements are needed to enhance the design.

e- Part 5 Ground Fault Current Determination

In order to compute the fault current, first \underline{Z}_P (over head lines impedance) and \underline{Z}_U (cables impedance) has to be determined as explained in Eq. (3-20). There are two overhead lines connected to grounding system and zero number of cables is connected to the system in the initialization of station operation. So \underline{Z}_U can be approximated as infinite. \underline{Z}_P is determined as $2,58\ \Omega$ for one overhead line from the steps introduced in Eq. (3-1). APPENDIX B gives all the details in calculation steps of \underline{Z}_P . For two overhead lines \underline{Z}_P is 1.29Ω .

\underline{Z}_E is determined as 0.99Ω . from R parallel to \underline{Z}_P configuration. APPENDIX C includes all necessary calculations.

Turkish 154kV system is configured for 31.5kA maximum fault current. Current reduction factor (r) from overhead lines computed and its numerical value is 0.65. From maximum fault current and r, fault current ($I_{E_{\text{tot}}}$) is determined as 20.4kA. Current division factor (S_f) is found as 0.233. Decrement factor (D_f) is found as 1.0313. From $I_{E_{\text{tot}}}$, S_f and D_f , I_G is computed as 4.8kA and GPR is computed as 20.4 kV. Resultant touch potential distribution is given in Figure 4.19.

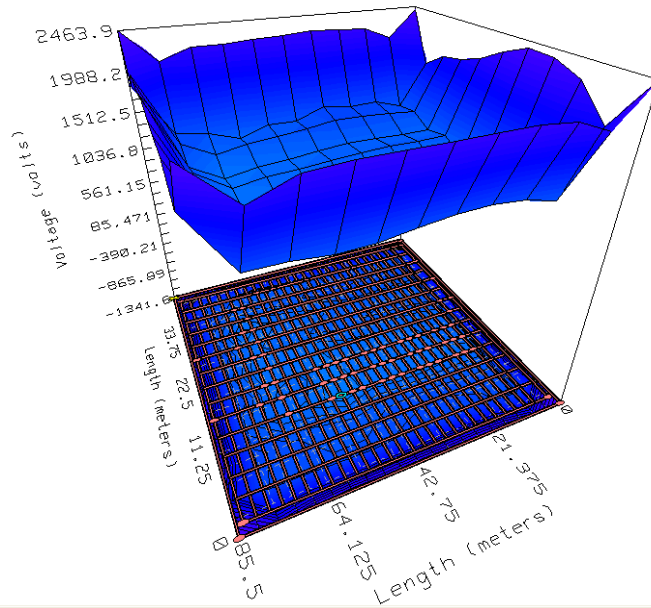


Figure 4.19: Touch potential distribution after overhead lines effect

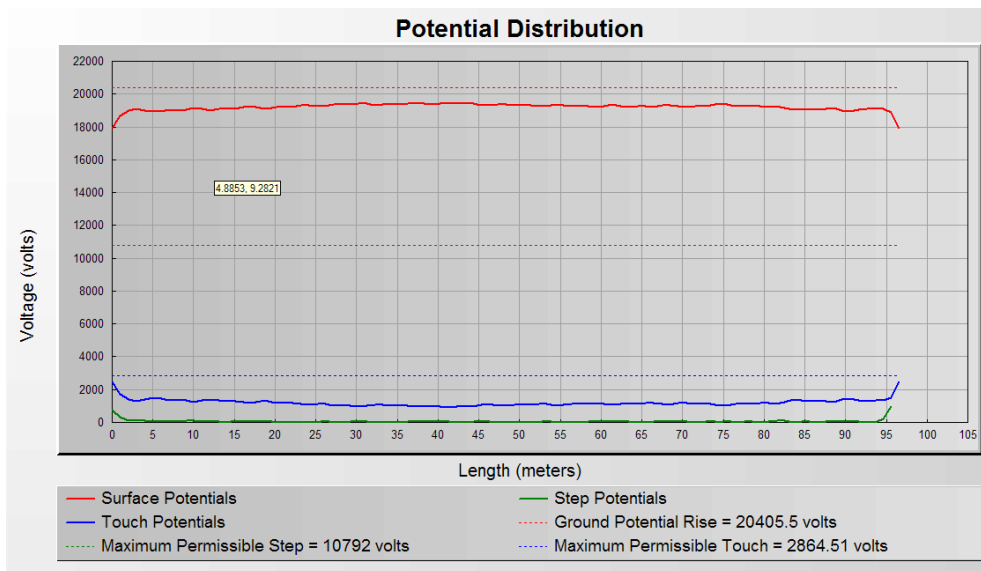


Figure 4.20: Potential distributions after overhead lines effect

Maximum permissible touch voltage is 2864.51 Volts. As shown in Figure 4.19, touch potential varies between 800 Volts and 2463.9 Volts. Therefore, touch voltage distribution is safe.

As shown in Figure 4.20, step and touch voltage criteria are satisfied. More over GPR is around 20kV and ground impedance decreases to 0.99Ω which is smaller than 1Ω . All grounding parameters are satisfied by addition of overhead lines effect in calculations. GPR reduction gain is about $((87493-20405)/87493*100)$ 76%.

As a result, overhead lines impedance effect on grounding is enormous and has to be calculated for all kind of grounding systems. Neglecting the calculation of this overhead line effect leads us to a non solution way even if all possible design improvements have been applied. Moreover, field engineers may include lots of unnecessary grounding equipment to satisfy design and regulation requirements by neglecting this effect, but problem remains in a non solution dilemma. In addition, in this kind of actual design problems, engineers try to find solutions which are not included in standards and literature such as parallel grid construction. Usage of these kinds of methods both decrease cost effectiveness. Parallel grid design is discussed next in a sample problem.

4.3.4. Actual Design Problem 3

Assume almost the same given data as previous problem (given in section “4.3.3 Actual Design Problem 2”) except, in this case, there are no overhead lines in the design. Instead 2x154kV cables are used. As mentioned in section “3.2 Current in the Grounding Systems” there is not an exact way to calculate effects of cables. So this problem leads to a non solution case without 154kV cable effects. This lack of formulations shows a new study title as “Determination of shielding and armoring cable effects on grounding grids”.

4.4. System Studies

In some problematic grounding design problems, conventional methods that are used with the omission of transmission line earth wires effect are not capable of achieving satisfactory designs as in the sample in section “4.3.3 Actual Design Problem 2”. For this kind of situations, engineers approach different methods such as parallel grid design, which is analyzed below.

a- Effect of Parallel Grid

In some actual grounding problems, ground resistance value cannot be lowered to desired values. It is a known fact that using two parallel equal resistances have an equivalent resistance of half one resistance. Taking this as an action point, engineers try to construct parallel grounding grids to achieve necessary requirements in their design. However, in actual cases, there is a mutual effect between these grids and this effect is large enough when systems are relatively close. Here, FEM analysis is used to investigate effecting parameters for parallel grounding grids, and determine necessary separation distances for different kind of grids. For this purpose, following actual grid problem is solved. A uniform soil model will be used in grounding problem of 154kV AC substation with the following given data in order to obtain ground resistance.

- Maximum fault current = 31,5 kA
- Fault Current Through the mat = 20 kA
- Minimum area of conductor = 120 mm² (minimum)
- Rod diameter (d) = 2,5 cm
- Rod Length (L) = 250 cm (minimum)
- Depth of conductors (h) = 50 cm (minimum)
- Step length = 1 m

- Fault Duration (t_s) = 0,5 s
- Human impedance = 1000 Ω
- Surface layer resistivity (Crushed rock) = 2500 $\Omega.m$ (maximum)
- Surface layer height = 15 cm
- 100m x 100m Grid size
- Second grid has the same configuration as this one.

Many simulations are prepared with different soil resistivity conditions and two of them are given in Table 4.6. Additional grid with the same size and parameters is sited with the separation of 0 to 3 times one region side and following data are taken from CYMGRD program.

As shown in Table 4.6, percentage of mutual effect is slightly dependant on resistivity of uniform soil but strongly dependent on separation distance of grids. Mutual effect is lower than 10 percent, when separation distance of square grids is about 3 times the one side length.

Consequently, from accuracy perspective, if the separation of grids are bigger than three times, this method can reduce ground resistance value to approximately %55 of the original grid which is a far effective value compared to addition of deep-driven-rods, rods and soil treatment around rods. However, construction of another grid with the same configuration yields to a doubled cost for the design of grounding grid. Moreover, in urban areas, land is so valuable and expansion of grounding is almost impossible. That is the factor avoiding this method to become a widely used solution.

Table 4.6: Parallel grid comparison table

One Grid Resistance (Ω)	Two Grids Parallel Resistance (Ω)	Separation of Grids (meter)	Percentage of Mutual Effect (%)
1000 Ω ·m Uniform Soil			
4,47	3,06	0,00	36,9
4,47	2,92	20,00	30,6
4,47	2,74	60,00	22,6
4,47	2,64	100,00	18,1
4,47	2,50	200,00	11,9
4,47	2,43	300,00	8,7
200 Ω ·m Uniform Soil			
0,89	0,61	0,00	37,1
0,89	0,58	20,00	30,3
0,89	0,55	60,00	23,6
0,89	0,52	100,00	16,9
0,89	0,50	200,00	12,4
0,89	0,48	300,00	7,9

CHAPTER 5

CONCLUSION

This thesis investigates possible design improvements for problematic grounding regions, which are high earth resistance and small area for grid applications, in AC-substation grounding design. These problematic cases such as inconsistent and high resistivity soil conditions cannot be resolved satisfactorily by the routine procedures of a field engineer that come from related standards (IEEE, IEE, Turkish National Regulations). Specifically, the design improvement items that are considered are (I) fault current determination, (II) soil treatment, (III) deep driven rods, (IV) explosion, and (V) parallel grid. In all of these techniques, the primary aim is to reduce both grounding resistance (R) and ground potential rise (GPR).

Each of the above design improvements are analyzed with finite element analysis and the results with the output of the related conventional methods. In this way, these analyses reveal the accuracy and cost effectiveness of design improvements. The following conclusions are made through this analysis for each design improvement item:

- I. Fault current determination: Both R and GPR reduction are possible up to %80 for the problematic cases considered in CHAPTER 4. In Turkey, engineers normally do not determine the fault current since in Turkish National Regulations, this current is specified as 20kA, irrespective of substation configuration. However, in most cases the grid current is much lower than this value. Lower currents prevent the utilization of

unnecessary grounding equipment, and therefore is very cost effective. From the accuracy perspective, this method gives best results for R and GPR reduction.

- II. Soil Treatment: There are two ways for soil treatment in AC substations. First one is soil treatment for the entire region. In this case, ground enhancement materials (GEM) are used to decrease resistivity of the region. Although effect of these materials are very much on R for high resistivity regions, GEM used in the region decreases as the time passes and additional GEM must be added to region for declared time periods in the design. Therefore, utilization of this kind of improvement increases maintenance costs. The second way to use soil treatment is filling GEM around rods. This method is almost useless for standard rods whereas effect of this method around deep driven rods can be enormous. According to the simulations done in CHAPTER 4, reduction on R made by deep driven rods without soil treatment is %6-8 percent lower than the soil treatment used case. This also means reduction on GPR is about %6-8.
- III. Deep driven rods: The aim of placing deep driven rods on the grounding grid design is to reach the lower resistivity layers under the ground. R and GPR reduction of this method is strictly dependant on lower resistivity layers. Its effectiveness on R and GPR rapidly increases when there exists low-resistivity lower layers in the grounding region. In the sample cases, considered reduction on R made by deep driven rods is about 15-20% reduction on R and GPR. Further, reduction is possible by use of soil treatment as explained in above paragraph.
- IV. Explosion: This method is based on the idea of using tree like electrodes in earth. There is no background information about this method in Turkey. Further, usage of this method may be expensive in Turkey conditions because of lack of know-how whereas its reduction effect on R value is gigantic. According to studies in [15], R reduction on a region can be reach to %80-90 percent.

- V. Parallel Grid: This method is based on the idea of constructing additional grounding grid near the main grounding design. The effect of this method decreases when two parallel grids are closer than 3 times one side length of equally designed grids. For this separation, R reduction is about %45 which seems as a good approach from accuracy perspective. However, cost of the grounding design is almost doubled when an additional grounding region and equipments installed far from the main grounding grid.

To conclude, the engineers are strongly advised to make the fault current calculation without omitting reduction factor and current division factor determinations for all of the specific grounding designs. Then, other enhancement methods given in CHAPTER 3 can be used to improve their design. Moreover, the results that are given here can be a guide to choose the particular improvement methods to achieve a safe and cost effective design.

The new GIS substations are within built-up areas, and therefore, the supply to these substations are with cables rather than overhead lines. Therefore, the division of current [18,27-30,32] between the grid system and the cable must be settled by experimental results. This is left as a future work.

REFERENCES

- [1] Raytheon Engineers & Constructors, Electric Distribution Systems Engineering Handbook, McGraw Hill, New York, 1994
- [2] “IEEE Guide for Safety in AC Substation Grounding”, IEEE Std. 80, USA, 2000
- [3] J. G. Sverak, “Simplified Analysis of Electrical Gradients above a Ground Grid; Part I – How good is the present IEEE method?”, IEEE Transactions on Power Apparatus and Systems, Vol. PAS-103, pp. 7-25, January 1984
- [4] S. J. Schwarz, “Analytical Expressions for the Resistance of Grounding Systems”, AIEE Transactions, Vol. 73 part III-B, pp.1011-1016, 1954
- [5] Beldev Thapar, Victor Gerez, Arun Balakrishnan, Donald A. Blank, “Evaluation of Ground Resistance of a Grounding Grid of Any Shape”, IEEE Transactions on Power Delivery, Vol. 6 No.2, April 1991
- [6] “The New IEEE Standard Dictionary of Electrical and Electronic Terms”, IEEE Std. 100, USA, 1992
- [7] “Definitions”, NEC Std. 100, USA, 1993
- [8] “IEEE Recommended Practice for Grounding of Industrial and Commercial Power Systems (IEEE Green Book)”, IEEE Std. 142, USA, 2007
- [9] K.C.Agrawal, Industrial Engineering and Applications Handbook, Newnes, Great Britain, 2001
- [10] Paul Gill, Electrical Power Equipment Maintenance and Testing, Marcel Dekker, New York, 1998
- [11] “IEEE Guide for Measuring Earth Resistivity, Ground Impedance, and Earth Surface Potentials of a Ground System.”, IEEE Std. 81, USA, 1983
- [12] J.A. Güemes, F.E. Hernando, “Method for Calculating the Ground Resistance of Grounding Grids Using FEM”, IEEE Transactions on Power Delivery, Vol. 19 No.2, April 2004

- [13] J.A. Güemes, F.E. Hernando, F. Rodrigez, J.M. Ruiz, "A Practical Approach of Determining the Ground Resistance of Grounding Grids", IEEE Transactions on Power Delivery, Vol. 21 No.3, July 2006
- [14] John D. Mcdonald, Electric Power Substations Engineering, CRC Press, New York, 2001
- [15] Qingbo Meng, Jinliang He, "A New Method to Decrease Ground Resistances of Substation Grounding Systems in High Resistivity Regions", IEEE Transactions on Power Delivery, Vol. 14 No. 3, July 1999
- [16] John Finn, IEE Substation Earthing - Shedding Light on The Black Art, IEE Seminar, Savoy Place London, 2000.
- [17] Roy B. Carpenter Jr., Mark M. Drabkin & Joseph A. Lanzoni, "Better Grounding", Lightning Eliminators & Consultants, Inc., USA, May 1997
- [18] "Currents during two separate simultaneous line-to-earth short-circuit currents flowing through earth", CEI IEC Std. 60909 – 3, November 2003
- [19] Takahiko Takashi, Taro Kawase, "Calculation of Earth Resistance For a Deep Driven Rod in a Multi Layer Earth Structure", IEEE Transactions on Power Delivery, Vol. 6 No. 2, July 1991
- [20] Rong ZENG, Jinliang HE, Zanji WANG, Yanqing GAO, "Analysis on Influence of Long Vertical Grounding Electrodes on Grounding System for Substation", Power System Technology, 2000. Proceedings. PowerCon 2000. International Conference on, Vol. 3, pp. 1475-1480, 2000
- [21] Turkish Government, "Grounding Regulations for Electrical Installations", The Official Gazette No. 24500, August 21, Turkey, 2001
- [22] Chem Rod, Lightning Eliminators & Consultants, Inc., <http://www.lightningeliminators.com>, January 25, 2009
- [23] ERICO Engineers, "Ground Enhancement Material (GEM)", ERICO, USA, 2005
- [24] Ioannis F. Gonos, Ioannis A. Stathopoulos, "Estimation of Multilayer Soil Parameters Using Genetic Algorithms", IEEE Transactions on Power Delivery, Vol. 20 No. 1, January 2005
- [25] F. P. Dawalibi, J. Ma, R. D. Southey "BEHAVIOUR OF GROUNDING SYSTEMS IN MULTILAYER SOILS:A PARAMETRIC ANALYSIS", IEEE Transactions on Power Delivery, Vol. 9 No. 1, January 1994

- [26] Hyung-Soo Lee, Jung-Hook Li-m, Farid P. Dawalibli, Jinxi Ma, "EFFICIENT GROUND GRID DESIGNS IN LAYERED SOILS", IEEE Transactions on Power Delivery, Vol. 13 No. 3, July 1998
- [27] Yin xia Shi, Hai qing Niu, Yao Zhang, Ze pei Yi, Xiao bing Wang and Yi gang Liu, "A New Method for Evaluating Fault Reduction Factor in HV Cable System", IEEE/PES Transmission and Distribution Conference & Exhibition: Asia and Pacific, Dalian, China, 2005
- [28] Stefano Mangione, "A Simple Method for Evaluating Ground-Fault Current Transfer at the Transition Station of a Combined Overhead-Cable Line", IEEE Transactions on Power Delivery, Vol. 23 No. 3, July 2008
- [29] I. Sarajevic, M. Majstrovic Senior Member, IEEE, "Determining Currents of Cable Sheaths by means of Current Load Factor and Current Reduction Factor", Power Tech Conference Proceedings, Vol. 3 pp. 4, Bologna, June 2003
- [30] Jovan M. Nahman, Vladimir B. Djordjevic, and Dragutin D. Salamon, "Grounding Effects of HV and MV Underground Cables Associated With Urban Distribution Substations", IEEE Transactions on Power Delivery, Vol. 17 No. 1, January 2002
- [31] Ljubivoje M. Popovic, "Determination of the Reduction Factor for Feeding Cable Lines Consisting of Three Single-Core Cables", IEEE Transactions on Power Delivery, Vol. 18 No. 3, July 2003
- [32] Bo Zhang, Xiang Cui, Senior Member, IEEE, Zhibin Zhao, Jinliang He, Senior Member, IEEE, and Lin Li, "Numerical Analysis of the Influence Between Large Grounding Grids and Two-End Grounded Cables by the Moment Method Coupled With Circuit Equations", IEEE Transactions on Power Delivery, Vol. 20 No. 2, April 2005

APPENDIX A

A.1 CYMGRD Program

CYMGRD is CYME's substation grounding grid design and analysis module specially designed to help engineers optimize the design of new grids and reinforce existing grids, of any shape, by virtue of easy to use, built-in danger point evaluation facilities . The program conforms to IEEE Std. 80-2000, Std. 81-1983 and Std. 837-2002.

Program details can be obtained from web address "www.cyme.com".

A.1.1 Program Features

The use of CYMGRD allows for the rapid analysis of various design alternatives to choose an economical solution for any particular installation. User-friendly data entry, efficient analysis algorithms and powerful graphical facilities render CYMGRD an efficient tool that helps the engineer arrive at technically sound and economical designs.

A.1.2 Analytical Capabilities

- Finite element analysis of the Ground Grid.
- Conductors, Rods and wire assembly.
- Computation of R and GPR (Ground Potential Rise).
- Touch and surface potential analysis, inside and outside the grid perimeter, with color display in 2D or 3D representation.

- Step voltage analysis.
- Uniform or Two-Layer Soil Model from field measurements or user-defined values.
- Computation of reduction factor (C_s).
- Library of the most common types of surface layer materials.
- Library of typical station soil resistivity values.
- Safety assessment calculations for maximum permissible Touch and Step Voltages as per IEEE 80-2000.
- Current Split Factor (S_F) estimated from substation configuration data as per IEEE Std. 80-2000.
- Computation of the Decrement Factor (D_F) from bus (X/R) ratio and shock duration data as per IEEE Std. 80-2000.
- DC component of asymmetrical fault current taken into account in the computations.
- Electrode analysis for the optimal sizing of Conductors and Rods based on the most common type of electrode
- material as per IEEE Std. 80-2000 and Std. 837-2002.
- Supports symmetrical or asymmetrical grids of any shape.
- Arbitrarily located ground Rods.
- Ability to model Return electrodes and Distinct electrodes.
- Ability to model concrete encased rods.
- Computation of maximum allowable single phase to ground fault current for a specified grid.

A.1.3 Screenshots of Data Entry

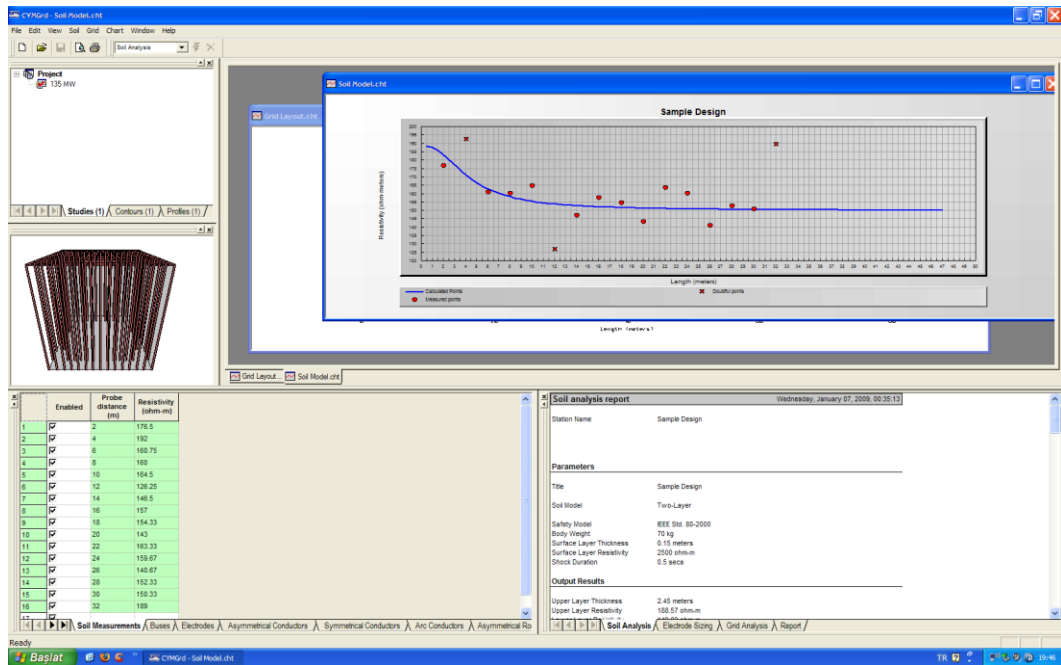


Figure A. 1: Full window screenshot

Enabled	Bus ID	LG Fault Current (amps)	Fault Duration (secs)	Remote Contribution (%)	LG X/R	Rtg (ohms)	Transmission Lines	Rdg (ohms)	Distribution Feeders
<input checked="" type="checkbox"/>	154 kV BB	20000	0.5	100	10	100	3	200	6
<input type="checkbox"/>									

Figure A. 2: Buses

	Enabled	Type	Material	Conductivity	Alpha Factor (1/C°)	Pr (μohm-m)	TCAP (J/cm3-°C)	Tm
1	<input type="checkbox"/>	Conductor	Copper anne	100	0.00393	1.72	3.42	1083
2	<input checked="" type="checkbox"/>	Conductor	Copper comm	97	0.00381	1.78	3.42	1084
3	<input type="checkbox"/>	Conductor	Copper_clad	40	0.00378	4.4	3.85	1084
4	<input type="checkbox"/>	Conductor	Copper_clad	30	0.00378	5.86	3.85	1084
5	<input type="checkbox"/>	Conductor	Aluminum EC	61	0.00403	2.86	2.56	657
6	<input type="checkbox"/>	Conductor	Aluminum 500	53.5	0.00353	3.22	2.6	652
7	<input type="checkbox"/>	Conductor	Aluminum 620	52.5	0.00347	3.28	2.6	654
8	<input type="checkbox"/>	Conductor	Aluminum_cla	20.3	0.0036	8.48	3.58	657
9	<input type="checkbox"/>	Rod	Copper_clad	20	0.00378	8.62	3.85	1084
10	<input checked="" type="checkbox"/>	Rod	Aluminum EC	61	0.00403	2.86	2.56	657
11	<input type="checkbox"/>	Rod	Aluminum 500	53.5	0.00353	3.22	2.6	652
12	<input type="checkbox"/>	Rod	Aluminum 620	52.5	0.00347	3.28	2.6	654
13	<input type="checkbox"/>	Rod	Steel 1020	10.8	0.0016	15.9	3.28	1510
14	<input type="checkbox"/>	Rod	Stainless clad	9.8	0.0016	17.5	4.44	1400
15	<input type="checkbox"/>	Rod	Zinc-coated s	8.6	0.0032	20.1	3.93	419
16	<input type="checkbox"/>	Rod	Stainless ste	2.4	0.0013	72	4.03	1400

Soil Measurements | Buses | **Electrodes** | Asymmetrical Conductors | Symmetrical Conductors | Arc Conductors | Asymmetrical Ro

Figure A. 3: Electrode types

	Enabled	Type	X1 (m)	Y1 (m)	X2 (m)	Y2 (m)	Grid Conductors parallel to X	Elements per Conductor parallel to X	Grid Conductors parallel to Y	Elements per Conductor parallel to Y	Depth (m)
1	<input checked="" type="checkbox"/>	Primary	0	0	74	50	17	20	25	20	0.5
2	<input checked="" type="checkbox"/>	Primary									

uses | Electrodes | Asymmetrical Conductors | **Symmetrical Conductors** | Arc Conductors | Asymmetrical Rods | Symmetrical Rods

Figure A. 4: Mat conductor entry

	X2 (m)	Y2 (m)	Rod rows parallel to X axis	Number of ground Rods per row	Length (m)	Depth (m)	Material	Size	Diameter (mm)	Material Encased	Material Thickness (mm)
1	74	50	9	2	2.5	0.5	Select		22	<input type="checkbox"/>	
2	68	50	2	13	2.5	0.5	Select		22	<input type="checkbox"/>	
3	62	44	2	11	2.5	0.5	Select		22	<input type="checkbox"/>	
4	68	36	5	2	2.5	0.5	Select		22	<input type="checkbox"/>	
5							Select			<input type="checkbox"/>	

Navigation: < > | uses \ Electrodes \ Asymmetrical Conductors \ Symmetrical Conductors \ Arc Conductors \ Asymmetrical Rods \ **Symmetrical Rods** /

Figure A. 5: Rod entry

A.1.4 Screenshots of Results

Soil analysis report		Wednesday, January 07, 2009, 00:35:13
Station Name	Sample Design	
Parameters		
Title	Sample Design	
Soil Model	Two-Layer	
Safety Model	IEEE Std. 80-2000	
Body Weight	70 kg	
Surface Layer Thickness	0.15 meters	
Surface Layer Resistivity	2500 ohm-m	
Shock Duration	0.5 secs	
Output Results		
Upper Layer Thickness	2.45 meters	
Upper Layer Resistivity	188.57 ohm-m	
Lower Layer Resistivity	149.83 ohm-m	
Reduction Factor Cs	0.786637	
Maximum Permissible Touch	877 volts	
Maximum Permissible Step	2841.91 volts	
RMS Error	8.88 %	

Figure A. 6: Soil analysis

Potential profile report		Monday, February 23, 2009, 20:04:17
Station Name	Sample Design	
Parameters		
Title	Potential profile plot #02	
Bus ID	154 kV BB	
LG Fault Current	20000 amps	
Remote Contribution	100 %	
Return Electrode Current	0 amps	
Parallel Z	2.52 ohms	
Upper Layer Thickness	2.45 meters	
Upper Layer Resistivity	188.57 ohm-m	
Lower Layer Resistivity	149.83 ohm-m	
Equal Potentials (Distinct)	Yes	
X1	0 meters	
Y1	0 meters	
X2	74 meters	
Y2	50 meters	
Step Interval	1 meters	
Potential Thresholds		
Ground Potential Rise	15728.6 volts	
Maximum Permissible Step	2841.91 volts	
Maximum Permissible Touch	877 volts	
Maximum		
Surface Potentials	14955.8 volts	
Step Potentials	506.61 volts	
Touch Potentials	2517.88 volts	

Figure A. 7: Potential results

APPENDIX B

B.1 Overhead Lines Impedance Z_p Determination

Data:

ENH type of protection cable OPGW (15,1 mm)

$$n = 1$$

$$\rho = 714 \Omega \cdot \text{m} \quad (\text{Lower layer resistivity})$$

$$d_W = 0,0 \text{ m} \quad (\text{For one grounding cable})$$

$$d_T = 300 \text{ m}$$

$$R_T = 20 \Omega$$

$$\#ENH = 2 \quad (\text{Number of Overhead lines})$$

$$\#ENH = 2 \quad (\text{Number of overheadlines used in calculations})$$

Formulations:

$$Z_p = (Z_W / 2) + [(Z_W / 2)^2 + Z_W \cdot R_T]^{1/2} \quad (\text{Eq. 54})$$

$$Z_W = Z'_W \cdot d_T \quad (\text{Eq. 58})$$

$$Z'_W = R'_W + (\omega\mu_0 / 8) + j\omega(\mu_0 / 2\pi) [(\mu_R / 4n) + \ln(\delta / r_{WW})] \quad (\text{Eq. 59})$$

$$\delta = 1,85 / (\omega\mu_0 / \rho)^{1/2} \quad (\text{Eq. 60})$$

Details of Formulations:

$$\omega\mu_0 = 0,40 \Omega/\text{km} \quad (\text{For 50 Hz})$$

$$r_{WW} = r_W \quad (\text{For one grounding cable})$$

$$r_{WW} = (r_W \cdot d_W)^{1/2} \quad (\text{For two grounding cable})$$

Results:

$$R'_W = 0,279 \Omega/\text{km}$$

$$\mu_R = 7,5$$

$$\delta = 2471,672$$

$$r_{WW} = 0,0076 \text{ m}$$

$$Z'_W = 0,329 + 0,927800606151553i$$

$$Z_W = 9,87E-002 + 0,278340181845466i$$

$$Z_W = 0,295 \Omega$$

$$Z_p = 2,58 \Omega \quad (\text{For one overhead line})$$

Solution:

$$Z_p = 1,29 \Omega \quad (\text{For two overhead lines})$$

APPENDIX C

C.1 I_G Determination

C.1.1 Determination of Z_E

$$\begin{aligned} R &= 4,24 \, \Omega \\ Z_U &= \text{N/A} && \text{(In the start of station operation cables are not connected)} \\ Z_P &= 1,29 \, \Omega && \text{(For two overhead lines)} \\ Z_E &= 0,99 \, \Omega && \text{(Equivalent Impedance of System Grounding)} \end{aligned}$$

C.1.2 Determination of I_{Etot}

Data:

$$d_{WL} = 9,5 \, \text{m}$$

Formulations:

$$r = 1 - (Z'_{WL} / Z'_W) \quad (\text{Eq. 50})$$

$$Z'_{WL} = (\omega\mu_0 / 8) + j\omega(\mu_0 / 2\pi) \cdot \ln(\delta / d_{WL}) \quad (\text{Eq. 50})$$

Details:

$$d_{WL} = (d_{WL1} \cdot d_{WL2} \cdot d_{WL2})^{1/3} \quad (\text{For one grounding cable})$$

$$d_{WL} = (d_{W1L1} \cdot d_{W1L2} \cdot d_{W1L2} \cdot d_{W2L1} \cdot d_{W2L2} \cdot d_{W2L2})^{1/6} \quad (\text{For two grounding cable})$$

Results:

$$Z'_{WL} = 5E-002+0,354047067224129i$$

$$r = 0,644050032129243-7,23296999210167E-002i$$

$$r = 0,65$$

$$I_{Etot} = 20,4 \, \text{kA}$$

C.1.3 Determination of I_G

Data:

$$I_{Etot} = 20,0 \text{ kA}$$

$$t_f = 0,50 \text{ s}$$

$$X/R = 10$$

Formulations:

$$I_g = S_f \cdot I_{Etot}$$

$$S_f = [(ZP//ZU)/(ZP//ZU+RG)]$$

$$I_G = D_f \cdot I_g$$

$$T_a = (X/R) / \omega$$

$$D_f = (1 + ((T_a/t_f) \cdot (1 - e^{(-2t_f/T_a)})))^{1/2}$$

Results:

$$S_f = 0,233$$

$$I_g = 4,7 \text{ kA}$$

$$T_a = 0,032 \text{ s}$$

$$D_f = 1,031339894$$

$$I_G = 4,8 \text{ kA}$$

C.1.4 Determination of GPR

$$GPR = I_G \cdot R_G$$

$$GPR = 20,4 \text{ kV}$$

APPENDIX D

D.1 Grounding Standards

The Official Gazette No. 24500 dated August 21, 2001, “Grounding Regulations for Electrical Installations” [21] is the published Turkish regulations which is predicting the necessary standards for AC substation grounding. Also this regulation authorize EN, HD, IEC ve VDE standards —published in Europe— for the topics, which are not included in Turkish regulations. AC substation grounding design procedures explain step-by-step in IEEE 80-2000 [2].

In this study following standard-documents are explored for necessary design improvements for AC substation grounding in Turkey:

- CEI IEC 60909 – 3, Currents during two separate simultaneous line-to-earth short-circuit currents flowing through earth [18]
- IEEE 80 – 2000, IEEE Guide for Safety in AC Substation Grounding [2]
- IEEE 142-2007, IEEE Recommended Practice for Grounding of Industrial and Commercial Power Systems (IEEE Green Book) [8]
- IEEE 81-1983, IEEE Guide for Measuring Earth Resistivity, Ground Impedance, and Earth Surface Potentials of a Ground System. [11]

D.2 Utility Practice in Turkey

In Turkey, practice of AC substation grounding is ruled by [21]. According to this document following specifications are given.

Supply of all materials and erection work of the overall grounding system for each 380 kV and 154 kV substations are ruled by the following specifications. Short circuit current will be assumed 31.5 kA for each 154 kV substation and 50 kA for

each 380 kV substation. In calculation of actual step & touch voltage, grid current flowing through ground grid should be taken at least 20 kA for 154 kV Substations and 35 kA for 380 kV Substations. Maximum fault clearing time is set to be 0.5 seconds for AC substation grounding in Turkey.

Measurement of earth resistance shall be carried out by using the Wenner-four-pin method after site leveling has been completed.

The cross sectional area of the main ground mat conductors shall be 120 mm². Bare stranded copper or copper-weld cables shall be used in the ground mat. Further details for determination of cable size are represented in [2].

The calculated grounding system resistance preferably shall not exceed 0.5 Ω for 380 kV Substations and 1 Ω for 154 kV Substations. After the ground mat has been installed, the earth resistance of the system shall be measured to verify that on every part of the switchyard, the grounding system resistance is in conformity with the specified values or below with respect to step and touch voltages.

In arriving at tolerable values of step and touch voltages, the following assumptions shall be made. Fault clearing time is taken to be 0.5 second. Body resistance is taken to be 1,000 Ω (hands to both feet and one foot to the other). To increase the contact resistance between the soil and the feet of people in the substation, on the earth's surface above the ground grid a 0.15m layer of crushed rock or gravel will be spread. The value of resistance for gravel or crushed rock will be assumed at most with 2500 $\Omega\cdot\text{m}$.

D.3 Effect of Soil Resistivity

Soil Characteristics mainly effect soil resistivity so ground resistance hugely effected by soil characteristics. Soil resistivity can be in the order of 10, 100, 1000

or 10000 $\Omega\cdot\text{m}$. Grounding design can be classified into two groups according to the value of soil resistivity which belongs to the area to be grounded. These are low resistivity case design and high resistivity case design.

D.3.1 Low Resistivity Case

10 and 100 $\Omega\cdot\text{m}$ case can be called as low resistivity soil case. [21] and [2] are covering all the necessary design procedures, steps and rules for low resistivity case.

D.3.2 High Resistivity Case

1000 and 10000 $\Omega\cdot\text{m}$ case can be called as high resistivity soil case. The information given in [21] and [2] are sometimes insufficient to lead a design. Mostly some of the predictions placed in [21] are avoiding the IEEE 80-2000 [2] steps to lead a design in high resistivity soil cases. For this kind of design problems, possible design improvements are explained in CHAPTER 3.

APPENDIX E

E.1 Grounding Parameters

There are some numerical parameters that are used to measure the quality of grounding. In order to investigate the problem of grounding these parameters are introduced next. Detailed derivations for grounding parameters are given in [2].

E.1.1 Tolerable Body Current Limit

An electric current, rather than voltage, through a human body may cause electrical shock and can badly damage vital organs of a human body. Known affects of an electrical shock can be listed as: muscular contraction, unconsciousness, fibrillation of the heart, respiratory nerve blockage and burning. The muscular contraction during the shock makes it difficult to release an energized object if held by the hand and can also make the breathing difficult. As a result of danger to human life, the answer of the question “How much current on a human being is dangerous?” is required.

As we all know, current can be expressed using two major properties such as frequency and magnitude. In order to understand the body limits of a current passing through body, one has to observe how current frequency and magnitude has to be limited. Research indicates that human body can tolerate up to 25Hz and 100mA current. [2] This leads us to the fact that humans are vulnerable to the currents even if in low voltage systems, which have characteristics such as 50Hz, 220V, several Amperes in Turkey. Following energy equation is used to explore body limits in numerical values.

Energy absorbed by the body can be given as:

$$S_B = I_B^2 t_s \quad (\text{E. 1})$$

where I_B is the rms magnitude of the body current in A, t_s is the duration of the current in seconds.

As you see, if t_s goes to zero, the equation will lead to zero for S_B . That means that if we minimize the duration of the fault, the absorbed energy which is responsible from health danger will be minimized.

Another research indicates that 99.5% of persons weighing 70kg survived when S_B is 0.0246pu according to ANSI. Dangerous body current can be computed as the following formulas in the order of 70kg and 50kg human.

$$I_B = \frac{0.157}{\sqrt{t_s}} \quad (\text{E. 2})$$

$$I_B = \frac{0.116}{\sqrt{t_s}} \quad (\text{E. 3})$$

E.1.2 Tolerable Body Voltage Limits

Body resistance parameters have to be observed before investigating body voltage limits. Once the resistance parameters are understood tolerable body voltage limits can be defined correctly. For more detail analysis, refer to [2]. Following graphs and definitions for Tolerable Body Voltage Limits are taken from [14].

a- Ground potential rise (GPR)

The maximum electrical potential that a substation grounding grid may reach relative to a distant grounding point assumed to be at the potential of remote earth. GPR is the product of the magnitude of the grid current, the portion of the fault current conducted to earth by the grounding system, and the ground grid resistance.

$$GPR = I_G R \quad (E. 4)$$

where I_G is fault current circulating on grounding grid in A, R is grid resistance in Ω .

Note: Determination of grid resistance is a complex procedure and researchers investigate many conventional methods. Also, finite element analysis can be used for determination of grid resistance. More detailed analysis on these methodologies is given in section 2.1 Grounding Methods.

b- Mesh voltage

It is the maximum touch voltage within a mesh of a ground grid.

c- Metal-to-metal touch voltage

It is the difference in potential between metallic objects or structures within the substation site that can be bridged by direct hand-to-hand or hand-to-feet contact.

Note: The metal-to-metal touch voltage between metallic objects or structures bonded to the ground grid is assumed to be negligible in conventional substations.

However, the metal-to-metal touch voltage between metallic objects or structures bonded to the ground grid and metallic objects inside the substation site but not bonded to the ground grid, such as an isolated fence, may be substantial.

In the case of gas-insulated substations, the metal-to-metal touch voltage between metallic objects or structures bonded to the ground grid may be substantial because of internal faults or induced currents in the enclosures.

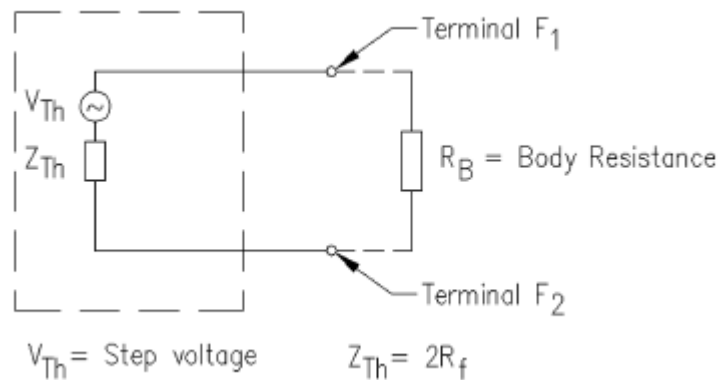


Figure E.1: Step voltage thevenin circuit ([2])

d- Step voltage

The difference in surface potential experienced by a person bridging a distance of 1 m with the feet without contacting any other grounded object.(Figure E.1)

If foot radius b is taken as 0.08m^2 , R_f can be rewritten as in Eq. (E. 5).

$$R_f = 6\rho C_s \tag{E. 5}$$

Body Tolerable voltage can be calculated from body resistance multiplied by the body current limit.

$$E_{S70} = (1000 + 6\rho C_s) \frac{0.157}{\sqrt{t_s}} \quad (\text{E. 6})$$

$$E_{S50} = (1000 + 6\rho C_s) \frac{0.116}{\sqrt{t_s}} \quad (\text{E. 7})$$

e- Touch voltage

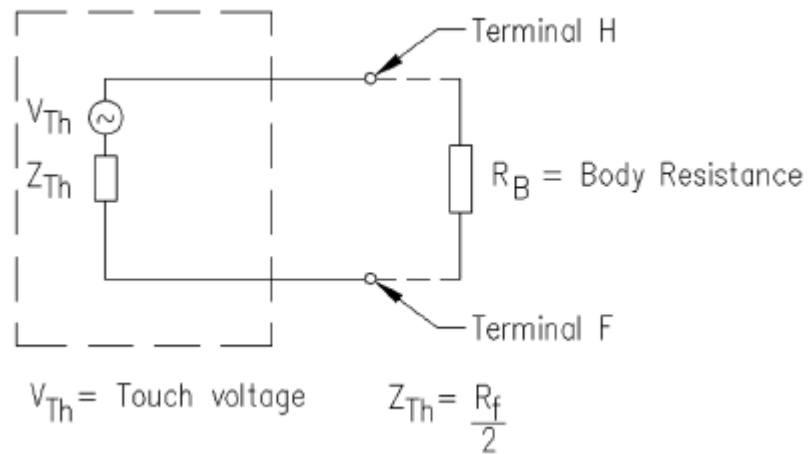


Figure E.2: Touch voltage thevenin circuit ([2])

The potential difference between the ground potential rise (GPR) and the surface potential at the point where a person is standing while at the same time having a hand in contact with a grounded structure. (Figure E.2)

If foot radius b is taken as 0.08m^2 , R_f can be rewritten in Eq. (E. 8). R_f for touch voltage condition is:

$$R_f = 1.5\rho C_s \quad (\text{E. 8})$$

Body Tolerable voltage can be calculated from body resistance multiplied by the body current limit.

$$E_{T70} = (1000 + 1.5\rho C_s) \frac{0.157}{\sqrt{t_s}} \quad (\text{E. 9})$$

$$E_{T50} = (1000 + 1.5\rho C_s) \frac{0.116}{\sqrt{t_s}} \quad (\text{E.10})$$

f- Transferred voltage

It is a special case of the touch voltage where a voltage is transferred into or out of the substation, from or to a remote point external to the substation site. The maximum voltage of any accidental circuit must not exceed the limit that would produce a current flow through the body that could cause fibrillation. These voltages are defined in Figure E.3.

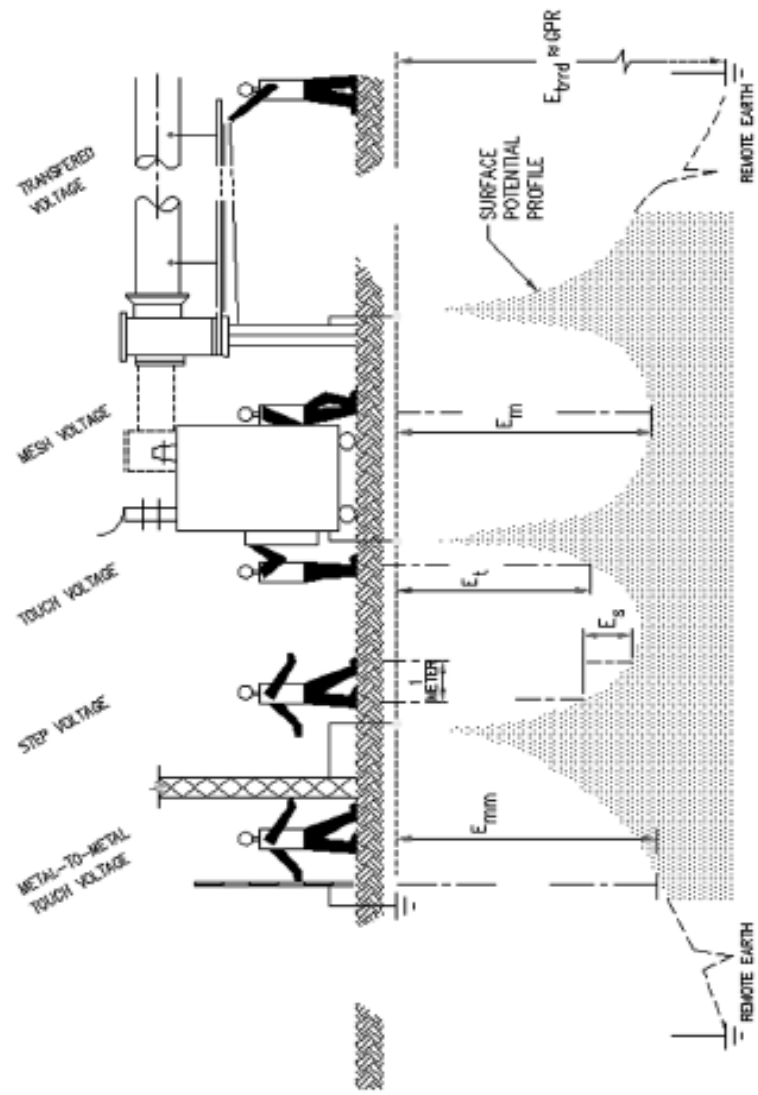


Figure E.3: Tolerable body voltage definitions ([2])